IEEE TRANSACTIONS ON

SYSTEMS, MAN, AND CYBERNETICS

PART B: CYBERNETICS

A PUBLICATION OF THE IEEE SYSTEMS, MAN, AND CYBERNETICS SOCIETY

Indexed in PubMed® and MEDLINE®, products of the United States National Library of Medicine

PubMed MEDLINE U.S. National Library of Medicine

DECEMBER 2012 VOLUME 42 NUMBER 6 ITSCFI (ISSN 1083-4419)

REGULAR PAPERS

IEEE

Approximate Optimal Control Design for Nonlinear One-Dimensional Parabolic PDE Systems Using Empirical Eigenfunctions and Neural Network

Biao Luo and Huai-Ning Wu

***Abstract*—This paper addresses the approximate optimal control problem for a class of parabolic partial differential equation (PDE) systems with nonlinear spatial differential operators. An approximate optimal control design method is proposed on the basis of the empirical eigenfunctions (EEFs) and neural network (NN). First, based on the data collected from the PDE system, the Karhunen–Loève decomposition is used to compute the EEFs. With those EEFs, the PDE system is formulated as a high-order ordinary differential equation (ODE) system. To further reduce its dimension, the singular perturbation (SP) technique is employed to derive a reduced-order model (ROM), which can accurately describe the dominant dynamics of the PDE system. Second, the Hamilton–Jacobi–Bellman (HJB) method is applied to synthesize an optimal controller based on the ROM, where the closed-loop asymptotic stability of the high-order ODE system can be guaranteed by the SP theory. By dividing the optimal control law into two parts, the linear part is obtained by solving an algebraic Riccati equation, and a new type of HJB-like equation is derived for designing the nonlinear part. Third, a control update strategy based on successive approximation is proposed to solve the HJB-like equation, and its convergence is proved. Furthermore, an NN approach is used to approximate the cost function. Finally, we apply the developed approximate optimal control method to a diffusion–reaction process with a nonlinear spatial operator, and the simulation results illustrate its effectiveness.**

***Index Terms*—Hamilton–Jacobi–Bellman (HJB) equation, Karhunen–Loève decomposition (KLD), neural network (NN), nonlinear parabolic partial differential equation (PDE) systems, optimal control, singular perturbation (SP).**

I. Introduction

OPTIMAL control theory is an important tool for controller synthesis. Up to the present, many powerful results on optimal control are available for linear or nonlinear lumped parameter systems (LPSs) which are described by ordinary differential equations (ODEs), such as the well-known Pontryagin maximum principle, the Bellman dynamic programming, and the linear quadratic (LQ) regulator (LQR) theory [1], [2]. However, in practice, a significant number of industrial processes are inherently distributed in space so that their behaviors depend on spatial position as well as time. These systems are usually described by a set of nonlinear partial differential equations (PDEs) with homogeneous or mixed boundary conditions. Due to the infinite-dimensional nature of these PDE systems, it is very difficult to directly use the optimal control design methods of LPSs to design an optimal controller that can be implemented in real time with reasonable computing power. Over the past decades, the optimal control theory of PDE systems has been developed by the pioneering works of Butkovskiy [3], Wang and Tung [4], and Lions [5] from a mathematical point of view, and more theoretical results can be found in [6] and [7]. Meanwhile, the optimal control problem of PDE systems has also been well studied from an engineering point of view, where considerable attention has been paid to methods that are based on the minimization of LQ performance indices.

Existing works on the optimal controller design of PDE systems can be classified into two types: *design-then-reduce* and *reduce-then-design* approaches. The former takes full advantage of infinite-dimensional operator theory to synthesize optimal controllers for the original PDE systems [8]–[10], and the resulting infinite-dimensional control solution is then lumped for implementation purposes. Curtain and Zwart [8] and Aksikas *et al.* [9] solved the LQ optimal control problem of infinite-dimensional state-space systems based on algebraic operator Riccati equations. Aksikas *et al.* [10] used spectral factorization to derive the feedback operator via the solution of an operator Diophantine equation. Ray [11] introduced the LQ optimal control method for linear parabolic PDE systems on the basis of the original PDE model, where the corresponding control gain operator was obtained by solving a Riccati differential equation. By contrast, the reduce-then-design approaches initially discretize the PDE system into an approximate finite-dimensional ODE model, which is then used for optimal control design purposes [12]–[19]. An input/output method was proposed to deal with the optimal concentration transition control problem of a certain type of distributed chemical reactors in [12], and two optimal control approaches were also developed for diffusion–convection–reaction processes in [13] by using discrete- and continuous-time LQR techniques. Xu *et al.* [14] considered a kind of bilinear parabolic PDE systems and used

Manuscript received May 15, 2011; revised December 5, 2011 and February 14, 2012; accepted April 5, 2012. Date of publication May 10, 2012; date of current version November 14, 2012. This work was supported in part by the National Basic Research Program of China (973 Program) under Grant 2012CB720003 and in part by the National Natural Science Foundation of China under Grants 61074057, 61121003, and 91016004. This paper was recommended by Editor E. Santos, Jr.

The authors are with the Science and Technology on Aircraft Control Laboratory, School of Automation Science and Electrical Engineering, Beihang University (formerly Beijing University of Aeronautics and Astronautics), Beijing 100191, China (e-mail: biao.luo@hotmail.com; whn@buaa.edu.cn).

Color versions of one or more of the figures in this paper are available online at http://ieeexplore.ieee.org.

Digital Object Identifier 10.1109/TSMCB.2012.2194781

an iterative scheme to construct a suboptimal controller based on the finite-dimensional ODE model. Sadek and Bokhari [15] employed finite interpolating orthogonal polynomials to approximate modal state variables for the optimal control problem of linear PDE systems. Ravindran [16] designed an optimal controller for the Navier–Stokes equation with the Newton method for the necessary condition of optimality. Approximate dynamic programming (ADP) was used by Yadav *et al.* [17] and Padhi *et al.* [18], [19] to synthesize suboptimal neurocontrollers. It is worth mentioning that the spatial differential operators (SDOs) of those PDE systems considered in the aforementioned works are usually linear [8]–[10], [12]–[19]. However, for many real industrial processes, the SDOs are nonlinear, such as the rapid thermal chemical vapor deposition process [11], [20], [21] and the nonlinear diffusion-reaction process (where the diffusion process is nonlinearly dependent on the thermal conductivity and temperature) [22], [23]. In this situation, it is desirable to develop optimal control design methods that deal with the problems of nonlinear SDOs.

When the SDO is nonlinear, the eigenvalue–eigenfunction problem of the spatial operator cannot be solved analytically in general; thus, it is difficult or impossible to obtain analytical basis functions. To overcome this limitation, some data-based methods have been used to obtain the so-called empirical eigenfunctions (EEFs), such as Karhunen-Loève decomposition (KLD) [14], [16]–[25] (which is also known as proper orthogonal decomposition or principal component analysis) and singular-value decomposition [26], [27]. Those EEFs can be employed to derive a finite-dimensional ODE system, which is then used for controller design. However, only few works concerned on optimal control, for example, Armaou and Christofides [22], converted the optimal control problem into a dynamic nonlinear programming problem with equality constraints, which was solved with reduced gradient techniques. Over the past decades, the Hamilton-Jacobi-Bellman (HJB) approach is proved to be an effective tool for the optimal control design of nonlinear systems, and some meaningful works have been done for LPSs. Nevertheless, it is still very difficult to solve the HJB equations either analytically or numerically until the present. In recent years, ADP [16]–[19], [28]–[36] has been used to deal with this problem in discrete formulation. ADP was proposed in [28], which has two basic structures: heuristic dynamic programming [29]–[33] and dual heuristic programming [31], [34]. Prokhorov and Wunsch [35] further gave more algorithms and presented a unified framework to all ADP types. One can refer to the special issue [36] for more results about the application of ADP in feedback control. For continuous systems, Saridis and Lee [37] developed an iterative approach to solve the HJB equation, but their work did not provide a method to estimate the cost function at each iterative step. Beard *et al.* [38], [39] suggested a successive approximation methodology, which solves the HJB equation by solving a series of linear generalized HJB (GHJB) equations with Galerkin approximation. Inspired by the works in [37]–[39], Abu-Khalaf and Lewis [40], [41] synthesized nearly optimal state feedback controllers for nonlinear continuous systems when there exist control constraints; Cheng *et al.* [42], [43] solved the time-varying HJB equation via neural network (NN) without policy iteration [42] and extended the approach to the case of constrained inputs [43]. However, to the best of the authors' knowledge, the optimal control problem of PDE systems with a nonlinear SDO is rarely studied in the framework of HJB equations.

In this paper, we synthesize a finite-dimensional approximate optimal controller for nonlinear parabolic PDE systems with a nonlinear SDO under the framework of HJB theory on the basis of the EEFs and NN. We initially use the KLD to compute the EEFs with the method of snapshots. The EEFs are subsequently applied to formulate the PDE system as a high-dimensional singular perturbation (SP) model of ODEs. By using the SP technique, a nonlinear reduced-order model (ROM) is derived, which captures the dominant (slow) dynamics of the PDE system. The ROM is then used as the basis for the optimal control design under the HJB framework, and the closed-loop asymptotic stability of the high-order ODE system is guaranteed. By dividing the optimal control law into two parts, a novel type of HJB-like equation is derived. To solve the HJB-like equation, a control update strategy based on successive approximation is proposed with the help of NN, and its convergence is proved. Finally, simulation studies are conducted on a nonlinear diffusion–reaction process to show the effectiveness of the approximate optimal controller synthesized in this paper.

Briefly speaking, the main contributions of this study include three aspects.

1) Develop a model reduction approach based on the KLD and the SP technique for parabolic PDE systems with a nonlinear SDO.
2) Propose an approximate optimal control method for nonlinear parabolic PDE systems under the framework of HJB theory, and derive a novel type of HJB-like equation. The asymptotic stability of the closed-loop high-order ODE system is proved by the SP technique.
3) Design a control update strategy to solve the HJB-like equation based on successive approximation and NN, and prove the convergence of this strategy.

The rest of this paper is arranged as follows. Section II gives the description of parabolic PDE systems. A ROM is derived via the KLD approach and the SP technique in Section III. The approximate optimal controller is synthesized and the related analyses are provided in Section IV. Section V presents the simulation studies on a nonlinear diffusion-reaction process, and Section VI gives a brief conclusion.

Notations: $\mathbb{R}$, $\mathbb{R}^n$, and $\mathbb{R}^{n\times m}$ are the set of real numbers, the n-dimensional Euclidean space, and the set of all real $n \times m$ matrices, respectively. $\langle\cdot,\cdot\rangle_{\mathbb{R}^n}$ and $\|\bullet\|$ denote the standard inner product and Euclidean norm in $\mathbb{R}^n$, respectively. For a symmetric matrix $\boldsymbol{M}$, $\boldsymbol{M} > (<)\ 0$ means that it is positive (negative) definite. $\overline{\sigma}(\cdot)$ and $\underline{\sigma}(\cdot)$ denote the maximum singular value and the minimum singular value of a matrix, respectively. The superscript T is used for the transpose. $\mathcal{L}^2([\underline{z},\overline{z}],\mathbb{R}^n)$ is the infinite-dimensional Hilbert space of n-dimensional square integrable vector function $\boldsymbol{\omega}(z) \in \mathbb{R}^n$, $z \in [\underline{z}, \overline{z}] \subset \mathbb{R}$, with the inner product and norm

$$\langle \boldsymbol{\omega}_1(\cdot), \boldsymbol{\omega}_2(\cdot) \rangle = \int_{\underline{z}}^{\overline{z}} \langle \boldsymbol{\omega}_1(z), \boldsymbol{\omega}_2(z) \rangle_{\mathbb{R}^n} \, dz$$

$$\|\boldsymbol{\omega}_1(\cdot)\|_2 = \langle \boldsymbol{\omega}_1(\cdot), \boldsymbol{\omega}_1(\cdot) \rangle^{\frac{1}{2}}$$

where $\boldsymbol{\omega}_1(\cdot)$ and $\boldsymbol{\omega}_2(\cdot)$ are any two elements of $\mathcal{L}^2([\underline{z}, \overline{z}], \mathbb{R}^n)$.

II. Description of Parabolic PDE Systems

In this paper, we consider a class of nonlinear parabolic PDE systems in one spatial dimension with the following state-space representation:

$$\boldsymbol{y}_t(z,t) = \boldsymbol{\mathcal{A}}(\boldsymbol{y}(z,t)) + \boldsymbol{f}(y(z,t)) + \boldsymbol{B}(z)\boldsymbol{u}(t) \quad (1)$$

subject to the boundary conditions

$$\begin{cases} \boldsymbol{M}_1 \boldsymbol{y}(\underline{z}, t) + \boldsymbol{N}_1 \, \boldsymbol{y}_z(z,t)|_{z=\underline{z}} = \boldsymbol{d}_1 \\ \boldsymbol{M}_2 \boldsymbol{y}(\overline{z}, t) + \boldsymbol{N}_2 \, \boldsymbol{y}_z(z,t)|_{z=\overline{z}} = \boldsymbol{d}_2 \end{cases} \quad (2)$$

and the initial condition

$$\boldsymbol{y}(z,0) = \boldsymbol{y}_0(z) \quad (3)$$

where $\boldsymbol{y}(z,t) = [y_1(z,t) \cdots y_n(z,t)]^{\mathrm{T}} \in \mathbb{R}^n$ is the state, the subscripts z and t stand for the partial derivatives with respect to z and t, respectively, i.e., $\boldsymbol{y}_t \triangleq \partial \boldsymbol{y}/\partial t$ and $\boldsymbol{y}_z \triangleq \partial \boldsymbol{y}/\partial z$, $z \in [\underline{z}, \overline{z}]$ is the spatial coordinate, $[\underline{z}, \overline{z}] \subset \mathbb{R}$ is the spatial domain of definition, and $t \in [0, \infty)$ is the temporal coordinate. $\boldsymbol{u}(t) \in \mathbb{R}^p$ is the manipulated input. $\boldsymbol{\mathcal{A}}(\boldsymbol{y})$ is a nonlinear parabolic SDO which involves first- and second-order spatial derivatives and locally satisfies the bound

$$\|\boldsymbol{\mathcal{A}}(\boldsymbol{y}_1) - \boldsymbol{\mathcal{A}}(\boldsymbol{y}_2)\|_2 \leq a_1 \|\boldsymbol{y}_1 - \boldsymbol{y}_2\|_2 + a_2 \|(\boldsymbol{y}_1 - \boldsymbol{y}_2)_z\|_2 + a_3 \|(\boldsymbol{y}_1 - \boldsymbol{y}_2)_{zz}\|_2 \quad (4)$$

where a_1, a_2, and a_3 are real positive constants. $\boldsymbol{f}(\boldsymbol{y})$ is a nonlinear vector function satisfying $\boldsymbol{f}(0) = 0$ and is locally Lipschitz continuous. $\boldsymbol{B}(z)$ is a known sufficient smooth matrix function of appropriate dimension which describes how control actions are distributed in spatial domains. $\boldsymbol{M}_1$, $\boldsymbol{N}_1$, $\boldsymbol{M}_2$, and $\boldsymbol{N}_2$ are constant matrices, $\boldsymbol{d}_1$ and $\boldsymbol{d}_2$ are constant vectors, and $\boldsymbol{y}_0(z)$ is the initial state. In this paper, we assume that the open- and closed-loop cases of the PDE system (1)–(3) are well posed. The well-posedness analysis of the PDE system (1)–(3) will involve complicated mathematical theory even for PDE systems with linear SDOs [44]. Since the main focus of this paper is on the controller design, we leave it for future investigation.

Denote the definition domain of the operator $\boldsymbol{\mathcal{A}}$ as

$$\begin{aligned} \mathcal{D}(\boldsymbol{\mathcal{A}}) \triangleq \Big\{ & \boldsymbol{y} \in \mathcal{L}^2([\underline{z}, \overline{z}], \mathbb{R}^n) \mid \\ & \boldsymbol{y}, \boldsymbol{y}_z, \boldsymbol{y}_{zz} \text{ are absolutely continuous}, \\ & \boldsymbol{\mathcal{A}}(\boldsymbol{y}) \in \mathcal{L}^2([\underline{z}, \overline{z}], \mathbb{R}^n), \\ & \boldsymbol{M}_1 \boldsymbol{y}(\underline{z}, t) + \boldsymbol{N}_1 \boldsymbol{y}_z(z,t)|_{z=\underline{z}} = \boldsymbol{d}_1, \\ & \boldsymbol{M}_2 \boldsymbol{y}(\overline{z}, t) + \boldsymbol{N}_2 \boldsymbol{y}_z(z,t)|_{z=\overline{z}} = \boldsymbol{d}_2 \Big\} \end{aligned}$$

and define the input operator as $\mathcal{B}\boldsymbol{u} = \boldsymbol{B}(z)\boldsymbol{u}(t)$; then, the nonlinear PDE system (1)–(3) can be simply reformulated as

$$\begin{cases} \boldsymbol{y}_t = \boldsymbol{\mathcal{A}}(\boldsymbol{y}) + \boldsymbol{f}(\boldsymbol{y}) + \mathcal{B}\boldsymbol{u} \\ \boldsymbol{y} \in \mathcal{D}(\boldsymbol{\mathcal{A}}) \\ \boldsymbol{y}(z,0) = \boldsymbol{y}_0(z). \end{cases} \quad (5)$$

III. Derivation of the Reduced-Order ODE System

Due to that the SDO of the PDE system (5) is nonlinear, it is impossible to compute the analytic expressions of the eigenvalues and eigenfunctions for the PDE system. Thus, they prohibit the direct use of model reduction methods, such as Galerkin's method and orthogonal collocation, with standard basis function sets to derive finite-dimensional approximations of the PDE system. To overcome this difficulty, we initially compute a set of EEFs (dominant spatial patterns) of the PDE system using KLD [24] with the method of snapshots. These EEFs, together with the SP technique, will be subsequently used to derive a ROM that accurately describes the dominant dynamics of the nonlinear PDE system.

A. Computation of EEFs With KLD

KLD is a popular statistical pattern analysis method for seeking the dominant structures in an ensemble of a high-dimensional process and obtaining low-dimensional approximate descriptions in many engineering fields. Given an ensemble of data, KLD yields a set of orthogonal EEFs for the representation of the ensemble, as well as a measure of the relative contribution of each EEF to the total "energy" (mean-square fluctuation) of the ensemble. In this sense, the EEFs provide an optimal basis for the truncated series representation, which has a smaller mean-square error than a representation by any other basis of the same dimension. In other words, the projection onto the first few EEFs captures most of the energy than any other projection. These properties make the EEFs a natural one to be considered when performing model reduction.

Now, we briefly present the procedure of KLD for computing EEFs with the method of snapshots in the context of nonlinear parabolic PDE systems. Collect M sampled states of the PDE system (5) (with $\boldsymbol{u} \equiv 0$), denoted as $\{\boldsymbol{y}_i(z)\}$ that is a sufficiently large set (which is called an ensemble). $\boldsymbol{y}_i(z)$, $i = 1, \ldots, M$, are typically called "snapshots" of the solution of (5). Assuming that snapshots $\{\boldsymbol{y}_i(z)\}$ collected from the PDE system (5) are ergodic [45], then, the spatial correlation function can be written as

$$\boldsymbol{R}(z,\xi) = \lim_{t \to \infty} \frac{1}{t} \int_0^t \boldsymbol{y}(z,\tau) \boldsymbol{y}^{\mathrm{T}}(\xi,\tau) d\tau$$

which is approximately calculated with

$$\boldsymbol{R}(z,\xi) = (1/M) \sum_{i=1}^{M} \boldsymbol{y}_i(z) \boldsymbol{y}_i^{\mathrm{T}}(\xi). \quad (6)$$

According to the Mercer theorem [46], $\boldsymbol{R}(z,\xi)$ has a property that

$$\boldsymbol{R}(z,\xi)=\sum_{i=1}^{\infty}\lambda_i\boldsymbol{\phi}_i(z)\boldsymbol{\phi}_i^{\mathrm{T}}(\xi)$$

where $\{\lambda_i\}$ represents nonzero eigenvalues and $\{\boldsymbol{\phi}_i(z)\}$ represents the corresponding orthogonal eigenfunctions of $\boldsymbol{R}(z,\xi)$. Considering the following integral

$$\begin{aligned}\int_{\underline{z}}^{\overline{z}}\boldsymbol{R}(z,\xi)\boldsymbol{\phi}_i(\xi)d\xi &= \int_{\underline{z}}^{\overline{z}}\sum_{j=1}^{\infty}\lambda_j\boldsymbol{\phi}_j(z)\boldsymbol{\phi}_i^{\mathrm{T}}(\xi)\boldsymbol{\phi}_i(\xi)d\xi\\ &=\lambda_i\boldsymbol{\phi}(z)\end{aligned} \tag{7}$$

and using (6), we have

$$\begin{aligned}\int_{\underline{z}}^{\overline{z}}\boldsymbol{R}(z,\xi)\boldsymbol{\phi}_i(\xi)d\xi &= \int_{\underline{z}}^{\overline{z}}\left(\frac{1}{M}\right)\sum_{i=1}^{M}\boldsymbol{y}_j(z)\boldsymbol{y}_j^{\mathrm{T}}(\xi)\boldsymbol{\phi}_i(\xi)d\xi\\ &=\sum_{j=1}^{M}\vartheta_j\boldsymbol{y}_j(z)\end{aligned} \tag{8}$$

where $\vartheta_j=(1/M)\int_{\underline{z}}^{\overline{z}}\boldsymbol{y}_j^{\mathrm{T}}(\xi)\boldsymbol{\phi}_i(\xi)d\xi$. From (7) and (8), we get

$$\boldsymbol{\phi}_i(z)=\sum_{j=1}^{M}\alpha_{ji}\boldsymbol{y}_j(z) \tag{9}$$

where $\alpha_{ji}=\lambda_i^{-1}\vartheta_j$.

Note that the EEFs $\{\boldsymbol{\phi}_i(z)\}$ are linear combinations of snapshots $\{\boldsymbol{y}_i(z)\}$; then, the essence to compute EEFs is reduced to compute the coefficients $\boldsymbol{\alpha}_i\triangleq[\alpha_{1i}\cdots\alpha_{Mi}]^{\mathrm{T}}$. Substituting (6) and (9) into (7) and rearranging (7) yield

$$\boldsymbol{Y}(z)(\boldsymbol{C}\boldsymbol{\alpha}_i)=\boldsymbol{Y}(z)(\lambda_i\boldsymbol{\alpha}_i) \tag{10}$$

where $\boldsymbol{C}\triangleq(c_{kj})_{M\times M}\in\mathbb{R}^{M\times M}$, $c_{kj}=(1/M)\int_{\underline{z}}^{\overline{z}}\boldsymbol{y}_k^{\mathrm{T}}(\xi)\boldsymbol{y}_j(\xi)d\xi$, and $\boldsymbol{Y}(z)\triangleq[\boldsymbol{y}_1(z)\cdots\boldsymbol{y}_M(z)]\in\mathbb{R}^{M\times M}$.

Assuming that the set $\{\boldsymbol{y}_i(z)\}$ is linearly independent, then, all eigenvectors $\{\boldsymbol{\alpha}_i\}$ and corresponding eigenvalues $\{\lambda_i\}$ can be computed by the standard method of eigenvalue decomposition for the following eigenvalue problem $\boldsymbol{C}\boldsymbol{\alpha}_i=\lambda_i\boldsymbol{\alpha}_i$. EEFs can be mutually orthogonal by normalizing the eigenvector $\boldsymbol{\alpha}_i$ to satisfy $\langle\boldsymbol{\alpha}_i,\boldsymbol{\alpha}_i\rangle_{\mathbb{R}^M}=1/(M\lambda_i)$. Then, all EEFs $\{\boldsymbol{\phi}_i(z)\}$ are directly computed by (9).

Remark 1: It is worth mentioning that the EEFs and corresponding eigenvalues are not eigenfunctions and eigenvalues of the operator $\boldsymbol{\mathcal{A}}(\boldsymbol{y})$ in the PDE system (5), i.e., $\boldsymbol{\mathcal{A}}(\boldsymbol{\phi}_i(z))\neq\lambda_i\boldsymbol{\phi}_i(z)$. An EEF denotes the "structure" that captures the coherence of the ensemble, and its eigenvalue is the corresponding energy that is captured.

B. Derivation of Reduced-Order ODE Model With SP Technique

Parabolic PDE systems are highly dissipative, and their main feature is that the eigenspectrum of the SDO can be partitioned into a finite-dimensional slow one and a stable fast complement. This implies that the dominant dynamic behavior of such systems can be accurately described by finite-dimensional slow systems [20], [21], [48]. However, the eigenspectrum of the nonlinear SDO is often unavailable. In fact, if the ensemble of snapshots is sufficiently large and contains sufficient information of the global dynamics of the PDE system, the use of EEFs for discretization of the PDE system is not fundamentally different from the use of other standard basis function sets (sine and cosine functions, Legendre polynomials, etc.) [21]. In [17]–[19], [21], and [22], Galerkin's method was employed to obtain a finite-dimensional ODE model based on EEFs by directly ignoring the fast modes. In this section, we derive a ROM based on EEFs by using the SP technique, which is essentially a multitime-scale approach. We first approximate the PDE system (5) with a high-order ODE model based on EEFs. To further reduce its dimension, an SP model of a coupled fast/slow ODE system is formulated, and a ROM is derived by introducing a fast time scale.

As is shown in Section III-A, $\{\lambda_i\}$ represents the eigenvalues of matrix $\boldsymbol{C}$, and $\{\boldsymbol{\phi}_i(z)\}$ represents the corresponding EEFs in KLD. Sorting $\{\lambda_i\}$ and $\{\boldsymbol{\phi}_i(z)\}$ with respect to $\{\lambda_i\}$ in a descending order, i.e., $\lambda_1\geq\lambda_2\geq\cdots\geq\lambda_M$, the solution $\boldsymbol{y}(z,t)$ of the PDE system (5) can be approximately represented as

$$\hat{\boldsymbol{y}}(z,t)\triangleq\sum_{i=1}^{M}x_i(t)\boldsymbol{\phi}_i(z). \tag{11}$$

Replacing $\boldsymbol{y}(z,t)$ in (5) with (11) and conducting inner product with EEFs on both sides of (5), we obtain an M-dimensional ODE system

$$\begin{cases}\dot{\boldsymbol{x}}=\tilde{\boldsymbol{A}}(\boldsymbol{x})+\tilde{\boldsymbol{f}}(\boldsymbol{x})+\tilde{\boldsymbol{B}}\boldsymbol{u}\\ \boldsymbol{x}(0)=\boldsymbol{x}_0\end{cases} \tag{12}$$

where $\boldsymbol{x}\triangleq[x_1\cdots x_M]^{\mathrm{T}}$, $\tilde{\boldsymbol{A}}(\boldsymbol{x})\triangleq\langle\boldsymbol{\mathcal{A}}(\hat{\boldsymbol{y}}),\boldsymbol{\Phi}(z)\rangle$, $\tilde{\boldsymbol{f}}(\boldsymbol{x})\triangleq\langle\boldsymbol{f}(\hat{\boldsymbol{y}}),\boldsymbol{\Phi}(z)\rangle$, $\tilde{\boldsymbol{B}}\triangleq\langle\boldsymbol{B}(z),\boldsymbol{\Phi}(z)\rangle$, and $\boldsymbol{x}_0\triangleq\langle\hat{\boldsymbol{y}}_0(z),\boldsymbol{\Phi}(z)\rangle$, with $\boldsymbol{\Phi}(z)\triangleq[\boldsymbol{\phi}_1(z)\cdots\boldsymbol{\phi}_M(z)]^{\mathrm{T}}$. From [20, Proposition 1], the discrepancy between the solution $\boldsymbol{y}(z,t)$ of the PDE system (5) and the solution $\hat{\boldsymbol{y}}(z,t)$ [obtained via (11) and (12)] satisfies $\|\boldsymbol{y}(z,t)-\hat{\boldsymbol{y}}(z,t)\|_2=\mu(M)$, where $\mu(M)$ is a small positive real number that depends on M and $\lim_{M\to\infty}\mu(M)=0$.

Due to the high dimension of the ODE system (12), a further dimension reduction is required. A linearization is conducted for (12) at the equilibrium point (i.e., the origin) of interest; then, (12) is equivalently rewritten as

$$\begin{cases}\dot{\boldsymbol{x}}=\boldsymbol{A}\boldsymbol{x}+\tilde{\boldsymbol{B}}\boldsymbol{u}+\tilde{\boldsymbol{g}}(\boldsymbol{x})\\ \boldsymbol{x}(0)=\boldsymbol{x}_0\end{cases} \tag{13}$$

where $\boldsymbol{A}\triangleq\partial[\tilde{\boldsymbol{A}}(\boldsymbol{x})+\tilde{\boldsymbol{f}}(\boldsymbol{x})]/\partial\boldsymbol{x}|_{\boldsymbol{x}=0}$ and $\tilde{\boldsymbol{g}}(\boldsymbol{x})\triangleq\tilde{\boldsymbol{A}}(\boldsymbol{x})+\tilde{\boldsymbol{f}}(\boldsymbol{x})-\boldsymbol{A}\boldsymbol{x}$.

Now, we equivalently rewrite (13) as a coupled ODE system with slow and fast subsystems of dimensions N and $M-N$, respectively

$$\begin{cases} \dot{\boldsymbol{x}}_s = \boldsymbol{A}_s\boldsymbol{x}_s + \boldsymbol{A}_{sf}\boldsymbol{x}_f + \boldsymbol{B}_s\boldsymbol{u} + \tilde{\boldsymbol{g}}_s(\boldsymbol{x}_s, \boldsymbol{x}_f) \\ \dot{\boldsymbol{x}}_f = \boldsymbol{A}_{fs}\boldsymbol{x}_s + \boldsymbol{A}_f\boldsymbol{x}_f + \boldsymbol{B}_f\boldsymbol{u} + \tilde{\boldsymbol{g}}_f(\boldsymbol{x}_s, \boldsymbol{x}_f) \\ \boldsymbol{x}_s(0) = \boldsymbol{x}_{s0} \\ \boldsymbol{x}_f(0) = \boldsymbol{x}_{f0} \end{cases} \tag{14}$$

where $\boldsymbol{x}_s \triangleq [x_1 \cdots x_N]^{\mathrm{T}} \in \mathbb{R}^N$, $\boldsymbol{x}_f \triangleq [x_{N+1} \cdots x_M]^{\mathrm{T}} \in \mathbb{R}^{M-N}$, $\tilde{\boldsymbol{g}}_s \triangleq [\tilde{g}_1 \cdots \tilde{g}_N]^{\mathrm{T}} \in \mathbb{R}^N$, $\tilde{\boldsymbol{g}}_f \triangleq [\tilde{g}_{N+1} \cdots \tilde{g}_M]^{\mathrm{T}} \in \mathbb{R}^{M-N}$, $[\boldsymbol{x}_s^{\mathrm{T}} \ \ \boldsymbol{x}_f^{\mathrm{T}}] = \boldsymbol{x}^{\mathrm{T}}$, $[\tilde{\boldsymbol{g}}_s^{\mathrm{T}} \ \ \tilde{\boldsymbol{g}}_f^{\mathrm{T}}] = \tilde{\boldsymbol{g}}^{\mathrm{T}}$, $[\boldsymbol{x}_{s0}^{\mathrm{T}} \ \ \boldsymbol{x}_{f0}^{\mathrm{T}}] = \boldsymbol{x}_0^{\mathrm{T}}$, and $\boldsymbol{A}_s$, $\boldsymbol{A}_{sf}$, $\boldsymbol{A}_{fs}$, $\boldsymbol{A}_f$, $\boldsymbol{B}_s$, and $\boldsymbol{B}_f$ are block matrices of appropriate dimensions that satisfy $\begin{bmatrix} \boldsymbol{A}_s & \boldsymbol{A}_{sf} \\ \boldsymbol{A}_{fs} & \boldsymbol{A}_f \end{bmatrix} = \boldsymbol{A}$ and $\begin{bmatrix} \boldsymbol{B}_s \\ \boldsymbol{B}_f \end{bmatrix} = \tilde{\boldsymbol{B}}$. The dimension (i.e., N) of the $\boldsymbol{x}_s$ subsystem should be chosen such that it satisfies

$$\sum_{i=1}^{N} \lambda_i \Big/ \sum_{j=1}^{M} \lambda_j \geq 1 - \zeta \tag{15}$$

for a small positive real number ζ. Let $\sigma(\boldsymbol{A}_s) = \{\tilde{\lambda}_1, \tilde{\lambda}_2, \ldots, \tilde{\lambda}_N\}$ be the eigenspectrum of $\boldsymbol{A}_s$ and $\sigma(\boldsymbol{A}_f) = \{\hat{\lambda}_1, \hat{\lambda}_2, \ldots, \hat{\lambda}_{M-N}\}$ be the eigenspectrum of $\boldsymbol{A}_f$. Then, the following assumption states our hypotheses for the separate property of (14).

Assumption 1:

1) $\mathrm{Re}\{\tilde{\lambda}_1\} \geq \mathrm{Re}\{\tilde{\lambda}_2\} \geq \cdots \geq \mathrm{Re}\{\tilde{\lambda}_N\}$ and $\mathrm{Re}\{\hat{\lambda}_1\} \geq \mathrm{Re}\{\hat{\lambda}_2\} \geq \cdots \geq \mathrm{Re}\{\hat{\lambda}_{M-N}\}$, where $\mathrm{Re}\{\tilde{\lambda}_j\}$ denotes the real part of $\tilde{\lambda}_j$.
2) $\mathrm{Re}\{\hat{\lambda}_1\} < 0$ and $|\mathrm{Re}\{\tilde{\lambda}_N\}|/|\mathrm{Re}\{\hat{\lambda}_1\}| = O(\varepsilon)$, where $\varepsilon \triangleq |\mathrm{Re}\{\tilde{\lambda}_1\}|/|\mathrm{Re}\{\hat{\lambda}_1\}| < 1$ is a small positive number.

Here, $O(\varepsilon)$ is the order-of-magnitude notation [47] (i.e., $\varsigma(\varepsilon) = O(\varepsilon)$ if there exist positive real numbers k_1 and k_2 such that $|\varsigma(\varepsilon)| \leq k_1|\varepsilon|, \forall|\varepsilon| \leq k_2$).

Remark 2: Like the parabolic PDE systems with linear SDOs [48], the parabolic PDE systems with nonlinear SDOs [20], [21] also have the fast/slow separation feature. Assumption 1 presented here is used to state this feature. By suitably choosing parameters N and M, the conditions in Assumption 1 are often satisfied for parabolic PDE systems.

From Assumption 1, we multiply both sides of the $\boldsymbol{x}_f$ subsystem with ε; then, a standard SP form of (14) can be equivalently given as

$$\begin{cases} \dot{\boldsymbol{x}}_s = \boldsymbol{A}_s\boldsymbol{x}_s + \boldsymbol{B}_s\boldsymbol{u} + \boldsymbol{g}_s(\boldsymbol{x}_s, \boldsymbol{x}_f) \\ \varepsilon\dot{\boldsymbol{x}}_f = \boldsymbol{A}_{f\varepsilon}\boldsymbol{x}_f + \varepsilon\boldsymbol{B}_f\boldsymbol{u} + \varepsilon\boldsymbol{g}_f(\boldsymbol{x}_s, \boldsymbol{x}_f) \\ \boldsymbol{x}_s(0) = \boldsymbol{x}_{s0} \\ \boldsymbol{x}_f(0) = \boldsymbol{x}_{f0} \end{cases} \tag{16}$$

where $\boldsymbol{A}_{f\varepsilon} \triangleq \boldsymbol{\varepsilon}\boldsymbol{A}_f$, $\boldsymbol{g}_s(\boldsymbol{x}_s, \boldsymbol{x}_f) \triangleq \boldsymbol{A}_{sf}\boldsymbol{x}_f + \tilde{\boldsymbol{g}}_s(\boldsymbol{x}_s, \boldsymbol{x}_f)$, and $\boldsymbol{g}_f(\boldsymbol{x}_s, \boldsymbol{x}_f) \triangleq \boldsymbol{A}_{fs}\boldsymbol{x}_s + \tilde{\boldsymbol{g}}_f(\boldsymbol{x}_s, \boldsymbol{x}_f)$.

Introducing a fast time scale $\tau = t/\varepsilon$ and setting $\varepsilon = 0$, then, the $\boldsymbol{x}_f$ subsystem in (16) is

$$\frac{\partial \boldsymbol{x}_f}{\partial \tau} = \boldsymbol{A}_{f\varepsilon}\boldsymbol{x}_f. \tag{17}$$

According to the fact that $\mathrm{Re}\{\hat{\lambda}_1\} < 0$ and the definition of ε, system (17) is globally exponentially stable, and then, we have that $\boldsymbol{x}_f = 0$. From (16), the ROM is obtained as

$$\begin{cases} \dot{\boldsymbol{x}}_s = \boldsymbol{A}_s\boldsymbol{x}_s + \boldsymbol{B}_s\boldsymbol{u} + \boldsymbol{g}_s(\boldsymbol{x}_s) \\ \boldsymbol{x}_s(0) = \boldsymbol{x}_{s0} \end{cases} \tag{18}$$

where $\boldsymbol{g}_s(\boldsymbol{x}_s) \triangleq \boldsymbol{g}_s(\boldsymbol{x}_s, 0)$.

Remark 3: The methodology developed here for derivation of the ROM is different from the method presented in [20]. In [20], the derivation of the coupled fast/slow ODE system (14) is based on a coordinate change, in which $\boldsymbol{A}_s$ and $\boldsymbol{A}_f$ are diagonal matrices, and the terms $\boldsymbol{A}_{sf}\boldsymbol{x}_f$ and $\boldsymbol{A}_{fs}\boldsymbol{x}_s$ are missing. However, the method probably generates complex system matrices (i.e., $\boldsymbol{A}_s$ and $\boldsymbol{A}_f$). This problem is circumvented in the proposed method by directly using the SP technique to the high-order ODE system (12).

IV. Approximate Optimal Controller Synthesis

In this section, based on the ROM (18), we will synthesize an approximate optimal controller for the PDE system (5) based on NN under the framework of HJB theory.

A. Optimal Controller Synthesis by HJB Approach

Let us consider a generalized performance functional

$$V(\boldsymbol{x}_{s0}) = \int_0^{+\infty} \left(Q(\boldsymbol{x}_s) + \boldsymbol{u}^{\mathrm{T}}\boldsymbol{R}\boldsymbol{u}\right) dt \tag{19}$$

where $Q(\boldsymbol{x}_s)$ is a positive definite function, i.e., $\forall\boldsymbol{x}_s \neq 0$, $Q(\boldsymbol{x}_s) > 0$; $Q(\boldsymbol{x}_s) = 0$ only when $\boldsymbol{x}_s = 0$. $\boldsymbol{R} \in \mathbb{R}^{p\times p}$ is a positive definite matrix. For $\boldsymbol{x}_s \in \Omega \subset \mathbb{R}^n$, $V(\boldsymbol{x}_s) \in C^1(\Omega)$ is a positive definite function, i.e., $\forall\boldsymbol{x}_s \neq 0, V(\boldsymbol{x}_s) > 0; V(\boldsymbol{x}_s) = 0$ only when $\boldsymbol{x}_s = 0$. We introduce the following definition of admissible control.

Definition 1 [37], [38] (Admissible Control): For the given system (18), with $\boldsymbol{x}_s \in \Omega$, a control $\boldsymbol{u}(\boldsymbol{x}_s) : \Omega \to \mathbb{R}^p$ is defined to be admissible with respect to (19) on Ω, denoted by $\boldsymbol{u}(\boldsymbol{x}_s) \in \mathcal{U}(\Omega)$, if the following hold: 1) $\boldsymbol{u}$ is continuous on Ω; 2) $\boldsymbol{u}(0) = 0$; 3) $\boldsymbol{u}(\boldsymbol{x}_s)$ stabilizes the system (18); and 4) $V(\boldsymbol{x}_{s0}) < \infty, \forall\boldsymbol{x}_{s0} \in \Omega$.

Our aim is to find an admissible control $\boldsymbol{u}^*(\boldsymbol{x}_s) \in \mathcal{U}(\Omega)$ that minimizes the performance functional (19). It is well known that the optimal control problem for a nonlinear system can be equivalently converted to solve the following HJB equation:

$$\inf_{\boldsymbol{u}\in\mathcal{U}(\Omega)} H(\boldsymbol{u}) = 0 \tag{20}$$

where $H(\boldsymbol{u})$ is the Hamilton function

$$H(\boldsymbol{u}) \triangleq \left(V_{\boldsymbol{x}_s}^*\right)^{\mathrm{T}} (\boldsymbol{A}_s\boldsymbol{x}_s + \boldsymbol{B}_s\boldsymbol{u} + \boldsymbol{g}_s) + Q + \boldsymbol{u}^{\mathrm{T}}\boldsymbol{R}\boldsymbol{u}$$

where V^* is the value function and the subscript $\boldsymbol{x}_s$ denotes the partial derivative with respect to $\boldsymbol{x}_s$, i.e., $V_{\boldsymbol{x}_s}^* \triangleq \partial V^*/\partial\boldsymbol{x}_s$. According to the first-order necessary condition of optimality, the optimal control $\boldsymbol{u}^*$ satisfies $\partial H(\boldsymbol{u})/\partial \boldsymbol{u}|_{\boldsymbol{u}=\boldsymbol{u}^*} = 0$, and thus, we have

$$\boldsymbol{u}^* = -\frac{1}{2}\boldsymbol{R}^{-1}\boldsymbol{B}_s^{\mathrm{T}} V_{\boldsymbol{x}_s}^*. \tag{21}$$

On the other hand, for an arbitrary control $\boldsymbol{u} \in \mathcal{U}(\Omega)$, the associated cost function V satisfies the following GHJB equation [37]–[39]:

$$(V_{\boldsymbol{x}_s})^{\mathrm{T}}(\boldsymbol{A}_s\boldsymbol{x}_s + \boldsymbol{B}_s\boldsymbol{u} + \boldsymbol{g}_s) + Q + \boldsymbol{u}^{\mathrm{T}}\boldsymbol{R}\boldsymbol{u} = 0. \tag{22}$$

Substituting $\boldsymbol{u}^*$ into (22) yields

$$\left(V_{\boldsymbol{x}_s}^*\right)^{\mathrm{T}}(\boldsymbol{A}_s\boldsymbol{x}_s + \boldsymbol{B}_s\boldsymbol{u}^* + \boldsymbol{g}_s) + Q + \boldsymbol{u}^{*\mathrm{T}}\boldsymbol{R}\boldsymbol{u}^* = 0. \tag{23}$$

Choosing V^* as the Lyapunov function candidate for the system (18), then, we have

$$\dot{V}^* = \left(V_{\boldsymbol{x}_s}^*\right)^{\mathrm{T}}(\boldsymbol{A}_s\boldsymbol{x}_s + \boldsymbol{B}_s\boldsymbol{u}^* + \boldsymbol{g}_s) = -Q - \boldsymbol{u}^{*\mathrm{T}}\boldsymbol{R}\boldsymbol{u}^* < 0. \tag{24}$$

This implies that the closed-loop system of (18) with optimal control $\boldsymbol{u}^*$ is asymptotically stable. From (21) and (23), the HJB equation (20) can be rewritten as

$$\left(V_{\boldsymbol{x}_s}^*\right)^{\mathrm{T}}(\boldsymbol{A}_s\boldsymbol{x}_s+\boldsymbol{g}_s)+Q(\boldsymbol{x}_s)-(1/4)\left(V_{\boldsymbol{x}_s}^*\right)^{\mathrm{T}}\boldsymbol{B}_s\boldsymbol{R}^{-1}\boldsymbol{B}_s^{\mathrm{T}}V_{\boldsymbol{x}_s}^*=0. \tag{25}$$

Therefore, the problem of designing an optimal control (21) is reduced to solve the HJB equation (25) for V^*.

We notice that the dynamics of the system (18) consists of two parts, the linear term $\boldsymbol{A}_s\boldsymbol{x}_s$ and the nonlinear term $\boldsymbol{g}_s$. In order to make full use of the linear part, in this paper, we develop an optimal controller synthesis method by using the following modal feedback control law:

$$\boldsymbol{u}(\boldsymbol{x}_s) = \boldsymbol{u}_1(\boldsymbol{x}_s) + \boldsymbol{u}_2(\boldsymbol{x}_s). \tag{26}$$

Let us consider the state penalty function $Q(\boldsymbol{x}_s)$ and the cost function $V(\boldsymbol{x}_s)$ of the following forms:

$$Q(\boldsymbol{x}_s) = \boldsymbol{x}_s^{\mathrm{T}}\boldsymbol{Q}_1\boldsymbol{x}_s + \tilde{Q}(\boldsymbol{x}_s) \tag{27}$$

$$V(\boldsymbol{x}_s) = \boldsymbol{x}_s^{\mathrm{T}}\boldsymbol{P}\boldsymbol{x}_s + \tilde{V}(\boldsymbol{x}_s) \tag{28}$$

where $\boldsymbol{Q}_1 > 0 \in \mathbb{R}^{n\times n}$, $\tilde{V}(\boldsymbol{x}_s) \in C^1(\Omega)$, and $\boldsymbol{P} > 0 \in \mathbb{R}^{n\times n}$ is the solution to the following algebraic Riccati equation (ARE):

$$\boldsymbol{A}_s^{\mathrm{T}}\boldsymbol{P} + \boldsymbol{P}\boldsymbol{A}_s + \boldsymbol{Q}_1 - \boldsymbol{P}\boldsymbol{B}_s\boldsymbol{R}^{-1}\boldsymbol{B}_s^{\mathrm{T}}\boldsymbol{P} = 0. \tag{29}$$

By substituting (28) into (21), the optimal controller can be equivalently written as

$$\boldsymbol{u}^* = \boldsymbol{u}_1^* + \boldsymbol{u}_2^* \tag{30}$$

where

$$\boldsymbol{u}_1^* \triangleq -\boldsymbol{R}^{-1}\boldsymbol{B}_s^{\mathrm{T}}\boldsymbol{P}\boldsymbol{x}_s \tag{31}$$

$$\boldsymbol{u}_2^* \triangleq -\frac{1}{2}\boldsymbol{R}^{-1}\boldsymbol{B}_s^{\mathrm{T}}\tilde{V}_{\boldsymbol{x}_s}^* \tag{32}$$

with $\boldsymbol{P}$ and $\tilde{V}^*$ to be determined. Using (26)–(29), it follows from (22) that a new type of GHJB-like equation is given as

$$(\tilde{V}_{\boldsymbol{x}_s})^{\mathrm{T}}(\overline{\boldsymbol{A}}_s + \boldsymbol{B}_s\boldsymbol{u}_2) + \overline{\boldsymbol{Q}} + \boldsymbol{u}_2^{\mathrm{T}}\boldsymbol{R}\boldsymbol{u}_2 = 0 \tag{33}$$

where $\overline{\boldsymbol{A}}_s \triangleq \boldsymbol{A}_s\boldsymbol{x}_s + \boldsymbol{B}_s\boldsymbol{R}^{-1}\boldsymbol{B}_s^{\mathrm{T}}\boldsymbol{P}\boldsymbol{x}_s + \boldsymbol{g}_s$ and $\overline{\boldsymbol{Q}} \triangleq \tilde{\boldsymbol{Q}} + 2\boldsymbol{x}_s^{\mathrm{T}}\boldsymbol{P}\boldsymbol{g}_s$. Replacing $\boldsymbol{u}_2$ in (33) with $\boldsymbol{u}_2^*$ that is given in (32) yields a new type of HJB-like equation

$$\left(\tilde{V}_{\boldsymbol{x}_s}^*\right)^{\mathrm{T}}\overline{\boldsymbol{A}}_s + \overline{\boldsymbol{Q}} - (1/4)\left(\tilde{V}_{\boldsymbol{x}_s}^*\right)^{\mathrm{T}}\boldsymbol{B}_s\boldsymbol{R}^{-1}\boldsymbol{B}_s^{\mathrm{T}}\tilde{V}_{\boldsymbol{x}_s}^* = 0. \tag{34}$$

It is easy to see [from (24)] that the synthesized optimal controller (30) [which is equal to (21)] can guarantee the closed-loop asymptotic stability of the ROM (18) and provide an optimal performance on the ROM. Theorem 1 shows that the closed-loop system of (12) is also asymptotically stable.

Theorem 1: Consider the nonlinear parabolic PDE system (5), for which Assumption 1 holds. Then, there exist positive real numbers δ_1, δ_2, and ε^*, such that, if $\|\boldsymbol{x}_{s0}\| \le \delta_1$, $\|\boldsymbol{x}_{f0}\| \le \delta_2$, and $\varepsilon \in (0, \varepsilon^*)$, the optimal controller (30) [or (21) equivalently] can guarantee that the closed-loop system of (12) is asymptotically stable.

Proof: See the Appendix.

Remark 4: Note that the optimal controller (30) can guarantee the asymptotic stability of the closed-loop system of (12); it follows from the fact that $\|\hat{\boldsymbol{y}}\|_2 = \|\boldsymbol{x}\| = \|\boldsymbol{x}_s\| + \|\boldsymbol{x}_f\|$ that the solution $\hat{\boldsymbol{y}}(z,t)$ [obtained via (11)] is asymptotically convergent. Furthermore, [20, Proposition 1] shows that the discrepancy between the solution $\boldsymbol{y}(z,t)$ of PDE system (5) and the solution $\hat{\boldsymbol{y}}(z,t)$ will tend to zero with the increase of M. In fact, owing to the parabolic nature of the SDO, the dominant dynamic behavior of parabolic PDE systems can be accurately described by a few modes. Many empirical studies [20]–[23] have also demonstrated that a very small M is enough to obtain a satisfactory result; that is to say, $\hat{\boldsymbol{y}}(z,t)$ and $\boldsymbol{y}(z,t)$ almost follow the same evolution properties. The optimal control synthesized for ROM (18) can achieve almost the same performance for the original PDE system (5).

Remark 5: Note that the first part $\boldsymbol{u}_1^*$ of the synthesized optimal controller of (30) is used to control the linear term of ROM (18). If the PDE system is linear or it works at the neighborhood of the equilibrium point, $\boldsymbol{u}_1^*$ is the theoretical optimal controller (when $\tilde{Q} = 0$); otherwise, if the PDE system is nonlinear, the second part $\boldsymbol{u}_2^*$ is employed to compensate the nonlinear dynamic $\boldsymbol{g}_s$.

B. Solving the HJB-like Equation via Control Update Strategy

Obviously, the problem of the optimal controller design is reduced to solve the HJB-like equation (34) for $\tilde{V}^*$. In this section, we will extend the works of Saridis and Lee [37] and

Beard *et al.* [39], to develop a control update strategy for the computation of $\tilde{V}^*$, which is given as follows.

Control update strategy:

Step 1: Given an initial control policy $\boldsymbol{u}_2^{(0)}$ such that $\boldsymbol{u}^{(0)} = \boldsymbol{u}_1 + \boldsymbol{u}_2^{(0)}$ in (26) is an admissible control, i.e., $\boldsymbol{u}^{(0)} \in \mathcal{U}(\Omega)$, let $i = 0$.

Step 2: With control policy $\boldsymbol{u}_2^{(i)}$, solve the following GHJB-like equation for $\tilde{V}^{(i+1)}$:

$$\left(\tilde{V}_{\boldsymbol{x}_s}^{(i+1)}\right)^{\mathrm{T}}\left(\overline{\boldsymbol{A}}_s+\boldsymbol{B}_s\boldsymbol{u}_2^{(i)}\right)+\overline{\boldsymbol{Q}}+\left(\boldsymbol{u}_2^{(i)}\right)^{\mathrm{T}}\boldsymbol{R}\boldsymbol{u}_2^{(i)}=0. \quad (35)$$

Step 3: Update the control policy $\boldsymbol{u}_2^{(i+1)}$ with

$$\boldsymbol{u}_2^{(i+1)} = -\frac{1}{2}\boldsymbol{R}^{-1}\boldsymbol{B}_s^{\mathrm{T}}\tilde{V}_{\boldsymbol{x}_s}^{(i+1)}. \quad (36)$$

Step 4: Set $i = i + 1$; if the terminate condition is not satisfied, go back to Step 2 and continue.

Observe that the control update strategy generates a sequence of pairs $(\tilde{V}^{(i)}, \boldsymbol{u}_2^{(i)})$, with $i = 1, 2, \ldots$. The following theorem can guarantee the convergence of the sequence.

Theorem 2: Let $(\tilde{V}^{(i)}, \boldsymbol{u}_2^{(i)})$, with $i = 1, 2, \ldots$, be a sequence of pairs which is generated through the aforementioned control update strategy; then

$$\tilde{V}^{(i)} \geq \tilde{V}^{(i+1)}, \qquad i = 1, 2, \ldots. \quad (37)$$

Furthermore, when $i \to \infty$, $\tilde{V}^{(i)} \to \tilde{V}^*$ and $\boldsymbol{u}_2^{(i)} \to \boldsymbol{u}_2^*$.

Proof: See the Appendix.

In the control update strategy, the successive approximation is used to solve the HJB-like equation (34) for $\tilde{V}^*$. However, in every update step, we should solve the GHJB-like equation (35) to obtain $\tilde{V}^{(i+1)}$. Therefore, in the next section, an approximate optimal controller is designed by using NN to estimate $\tilde{V}^{(i+1)}$.

C. Approximate Optimal Control Based on NN

From the well-known high-order Weierstrass approximation theorem [49], it follows that a continuous function can be uniformly approximated to any degree of accuracy by a set of linearly independent basis functions. Let $\boldsymbol{\gamma}(\boldsymbol{x}_s) = [\gamma_1(\boldsymbol{x}_s)\ \gamma_2(\boldsymbol{x}_s)\ \cdots\ \gamma_L(\boldsymbol{x}_s)]^{\mathrm{T}}$ be a set of linearly independent activation functions of the NN, where L is the number of neurons in the NN hidden layer. Then, for an iterative step in the control update strategy, the function $\tilde{V}^{(i+1)}$ can be estimated with NN approximation $\hat{V}^{(i+1)}$ as follows:

$$\hat{V}^{(i+1)} = \sum_{j=1}^{L} w_{i+1}^j \gamma_j(\boldsymbol{x}_s) = \boldsymbol{w}_{i+1}^{\mathrm{T}}\boldsymbol{\gamma}(\boldsymbol{x}_s) \quad (38)$$

where $\boldsymbol{w}_{i+1} = [w_{i+1}^1\ w_{i+1}^2\ \cdots\ w_{i+1}^L]^{\mathrm{T}}$ is the weight vector.

Remark 6: According to the Weierstrass approximation theorem, when $L \to \infty$, $\hat{V}^{(i+1)} \to \tilde{V}^{(i+1)}$. The influence of the NN approximation error on the controller design and closed-loop system stability is beyond the scope of this study, which is left for our future research. In this paper, we assume that the size L is large enough so that $\boldsymbol{\gamma}(\boldsymbol{x}_s)$ can accurately estimate $\tilde{V}^{(i+1)}$.

Replacing $\tilde{V}^{(i)}$ in (35) with $\hat{V}^{(i)}$ of (38) results in a residual error

$$e_N(\boldsymbol{x}_s)=\boldsymbol{w}_{i+1}^{\mathrm{T}}\boldsymbol{\gamma}_{\boldsymbol{x}_s}\left(\overline{\boldsymbol{A}}_s+\boldsymbol{B}_s\boldsymbol{u}_2^{(i)}\right)+\overline{\boldsymbol{Q}}+\left(\boldsymbol{u}_2^{(i)}\right)^{\mathrm{T}}\boldsymbol{R}\boldsymbol{u}_2^{(i)} \quad (39)$$

where the subscript $\boldsymbol{x}_s$ stands for the partial derivative with respect to $\boldsymbol{x}_s$, i.e., $\boldsymbol{\gamma}_{\boldsymbol{x}_s} \triangleq \partial\boldsymbol{\gamma}(\boldsymbol{x}_s)/\partial\boldsymbol{x}_s$. The weight vector $\boldsymbol{w}_{i+1}$ is determined by setting the projection of the error (39) on the basis functions $\boldsymbol{\gamma}(\boldsymbol{x}_s)$ to zero, i.e.,

$$\langle e_N(\boldsymbol{x}_s), \gamma_j(\boldsymbol{x}_s)\rangle_\Omega = 0, \qquad j = 1, \ldots, L \quad (40)$$

where $\langle e_N(\boldsymbol{x}_s), \gamma_j(\boldsymbol{x}_s)\rangle_\Omega = \int_\Omega e_N(\boldsymbol{x}_s)\gamma_j(\boldsymbol{x}_s)d\boldsymbol{x}_s$ is an inner product. Using (39), (40) can be written compactly in a matrix form as

$$\boldsymbol{\Theta}_i\boldsymbol{w}_{i+1} = -\boldsymbol{\sigma}_i, \qquad i = 0, 1, 2, \ldots \quad (41)$$

where $\boldsymbol{\Theta}_i \triangleq \langle\boldsymbol{\gamma}_{\boldsymbol{x}_s}(\overline{\boldsymbol{A}}_s + \boldsymbol{B}_s\boldsymbol{u}_2^{(i)}), \boldsymbol{\gamma}\rangle_\Omega \in \mathbb{R}^{L\times L}$ and $\boldsymbol{\sigma}_i \triangleq \langle\overline{\boldsymbol{Q}} + (\boldsymbol{u}_2^{(i)})^{\mathrm{T}}\boldsymbol{R}\boldsymbol{u}_2^{(i)}, \boldsymbol{\gamma}\rangle_\Omega \in \mathbb{R}^{L}$.

Since $\boldsymbol{\gamma}(\boldsymbol{x}_s)$ is independent, then $\boldsymbol{\Theta}_i$ is invertible [38]. Thus, from (41), we have

$$\boldsymbol{w}_{i+1} = -\boldsymbol{\Theta}_i^{-1}\boldsymbol{\sigma}_i. \quad (42)$$

By (36) and (38), $\boldsymbol{u}_2^{(i+1)}$ is approximately updated by

$$\boldsymbol{u}_2^{(i+1)}=-\frac{1}{2}\boldsymbol{R}^{-1}\boldsymbol{B}_s^{\mathrm{T}}\boldsymbol{\gamma}_{\boldsymbol{x}_s}^T\boldsymbol{w}_{i+1}, \qquad i=0, 1, 2, \ldots. \quad (43)$$

It can be seen that the control update strategy turns out to be an NN weight recursive iteration procedure between (42) and (43). The initial admissible control $\boldsymbol{u}_2^{(0)}$ is given by choosing an initial weight vector $\boldsymbol{w}_0$, which is often based on experience. Let $\boldsymbol{w}^*$ be the optimal weight vector for approximating the solution $\tilde{V}^*$ of the HJB-like equation (34). Then, the expression of (30) gives the approximate NN-based optimal control law

$$\boldsymbol{u}^* = -\boldsymbol{R}^{-1}\boldsymbol{B}_s^{\mathrm{T}}\boldsymbol{P}\boldsymbol{x}_s - (1/2)\boldsymbol{R}^{-1}\boldsymbol{B}_s^{\mathrm{T}}\boldsymbol{\gamma}_{\boldsymbol{x}_s}^T\boldsymbol{w}^*. \quad (44)$$

V. Simulation Studies

In this section, we give simulation studies on a nonlinear diffusion-reaction process [22], in which the SDO is nonlinear (i.e., the diffusion process is nonlinearly dependent on the thermal conductivity and temperature). This process is described with the following nonlinear parabolic PDE:

$$y_t=(k(y)y_z)_z+\beta_T(z)(e^{-\gamma/(1+y)}-e^{-\gamma})+\beta_U\,(b(z)u(t)-y) \quad (45)$$

subject to the Dirichlet boundary condition

$$y(0,t) = y(\pi,t) = 0 \quad (46)$$

and the initial condition

$$y(z,0) = y_0(z) \quad (47)$$

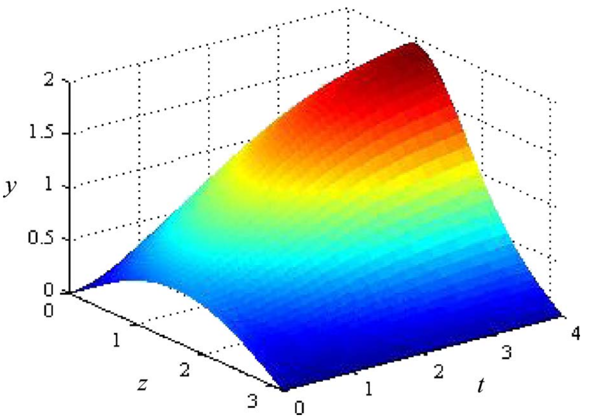

Fig. 1. Open-loop system state profile with the initial condition $y_0(z) = 0.5\sin(z)$.

where $y(z,t) \in (1, +\infty]$ is the state and $z \in [0, \pi]$. $k(y)$ is the diffusion coefficient which is nonlinearly dependent on the state, $\beta_T(z)$ is the heat of reaction which is spatially varying, β_U is the heat transfer coefficient, γ is the activation energy, and $b(z)$ is the actuator distribution function. Here, the process parameters are selected as follows:

$$\begin{aligned} k(y) &= 0.5 + 0.7/(y+1) \\ \beta_T(z) &= 12\,(\cos(z) + 1) \\ \beta_U &= 2 \\ \gamma &= 2 \\ b(z) &= H(z - 0.1\pi) - H(z - 0.5\pi) \end{aligned}$$

where $H(\bullet)$ is the standard Heaviside function. Moreover, it is easy to verify that the PDE system (45)–(47) satisfies the conditions in the system description in Section II. The PDE system (45)–(47) is often used to describe the typical thermal process in the chemical industry, such as catalytic rod [22], [23], wherein the thermal conductivity is a nonlinear function of temperature. Fig. 1 gives the state profile of the open-loop system with the initial condition $y_0(z) = 0.5\sin(z)$, which shows that the steady-state profile $y(z,t) = 0$ is an unstable one.

To compute the EEFs, we conduct an open-loop simulation on the PDE system and collect 1500 $(M = 1500)$ snapshots for the KLD procedure. Fig. 2 shows the first two EEFs. We find that the first two EEFs account for more than 99.0% energy contained in the ensemble of snapshots (i.e., $(\lambda_1 + \lambda_2)/\sum_{i=1}^{M}\lambda_i > 99.0\%$). Therefore, the PDE system can be accurately represented by a two-order ODE system (i.e., $N = 2$). The eigenspectra of $\boldsymbol{A}_s$ and $\boldsymbol{A}_f$ are $\sigma(\boldsymbol{A}_s) = \{0.7760, -3.9358\}$ and $\sigma(\boldsymbol{A}_f) = \{-11.4619, -17.0426, \ldots\}$, respectively. This means that Assumption 1 is satisfied for $\varepsilon = 0.0677$. By the method in Section III-B, the following ROM can be obtained:

$$\begin{cases} \dot{\boldsymbol{x}}_s = \begin{bmatrix} 0.8019 & -0.2088 \\ 0.5875 & -3.9617 \end{bmatrix} \boldsymbol{x}_s + \begin{bmatrix} 3.4218 \\ 1.6768 \end{bmatrix} u + \boldsymbol{g}_s(\boldsymbol{x}_s) \\ \boldsymbol{x}_s(0) = [\,2.0300 \quad -0.8370\,]^{\mathrm{T}} \end{cases} \tag{48}$$

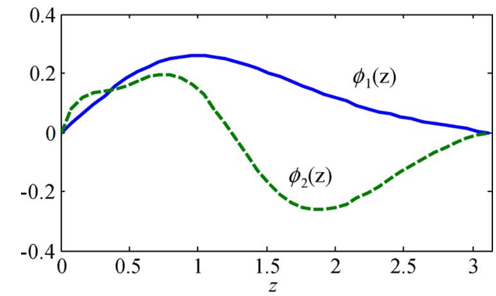

Fig. 2. First two EEFs generated by KLD.

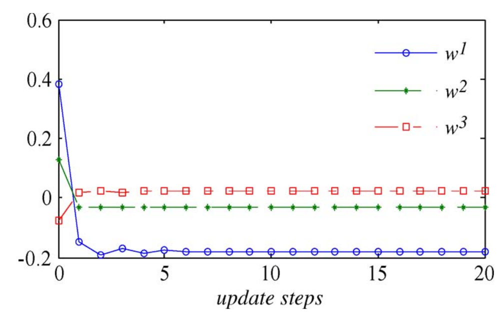

Fig. 3. Weights at each update step.

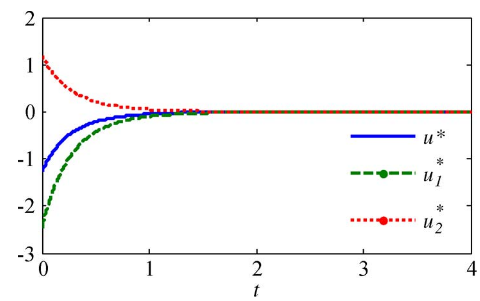

Fig. 4. Control actions u_1^*, u_2^*, and u^*.

where $\boldsymbol{x}_s = [x_1 \quad x_2]^{\mathrm{T}}$. Select the state penalty function $Q(\boldsymbol{x}_s) = \boldsymbol{x}_s^{\mathrm{T}}\boldsymbol{x}_s$ and the weighting matrix $\boldsymbol{R} = 1$ in performance functional (19)$\boldsymbol{Q}_1 = \boldsymbol{I}$ in (27). Solving the ARE (29), we get

$$\boldsymbol{P} = \begin{bmatrix} 0.3846 & -0.0366 \\ -0.0366 & 0.1272 \end{bmatrix}.$$

In order to estimate the function $\tilde{V}^*$, the activation function set for the NN is selected as $\boldsymbol{\gamma}(\boldsymbol{x}_s) = [x_1^2 \; x_2^2 \; x_1 x_2]^T$ with the size of $L = 3$, and the control update strategy is iterated 20 steps (i.e., terminate iteration after 20 steps). Fig. 3 shows the weights at each step. It can be observed from Fig. 3 that the weights converge to $\boldsymbol{w}^* = [-0.1798 \; -0.03007 \; 0.02129]^{\mathrm{T}}$.

With the aforementioned matrix $\boldsymbol{P}$ and weight vector $\boldsymbol{w}^*$, the approximate NN-based optimal control law is obtained via (44), which is applied to control the original PDE system (45)–(47). Figs. 4–6 show the simulation results. Fig. 4 shows the control actions, where $u_1^* = -\boldsymbol{R}^{-1}\boldsymbol{B}_s^{\mathrm{T}}\boldsymbol{P}\boldsymbol{x}_s$ and $u_2^* = -(1/2)\boldsymbol{R}^{-1}\boldsymbol{B}_s^{\mathrm{T}}\boldsymbol{\gamma}_{\boldsymbol{x}_s}^T\boldsymbol{w}^*$. The computed performance

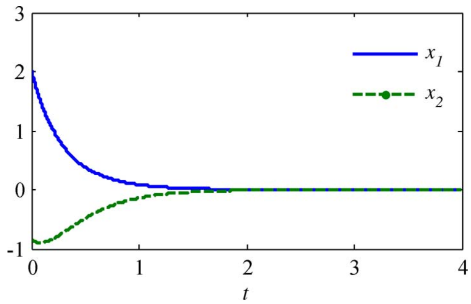

Fig. 5. Actual state trajectories of the closed-loop ROM.

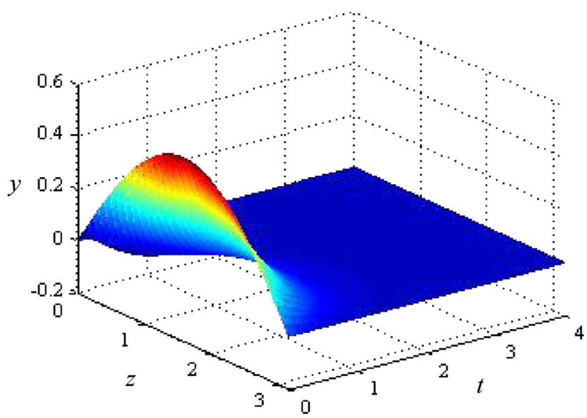

Fig. 6. State profile of the closed-loop PDE system.

index is $V^*(\boldsymbol{x}_{s0}) = 1.0004$, and Fig. 5 shows the actual state trajectories of the closed-loop ROM, where we can see that the states converge to the origin as time increases. Fig. 6 demonstrates the state profile of the closed-loop PDE system, which shows that the state profile quickly converges to the steady-state profile $y(z,t) = 0$.

VI. Conclusion

In this paper, an approximate optimal controller has been synthesized for a class of nonlinear parabolic PDE systems under the framework of HJB theory. Due to that the SDO of the PDE system is nonlinear, the data-based KLD approach and SP technique are used to derive a ROM, which can accurately describe the dominant dynamics of the PDE system. In order to make full use of the linear part of the ROM, the approximate optimal controller is given by two parts, and the closed-loop asymptotic stability of the high-order ODE system is guaranteed. The first part of the synthesized controller is developed for the linear part of the ROM, which is obtained by solving an ARE. On the other hand, the second part is employed to compensate the nonlinear dynamics, which is computed by solving a derived HJB-like equation. A control update strategy is also provided to solve the HJB-like equation by successive approximation, in which NN is employed to estimate the cost function. Finally, using a nonlinear diffusion–reaction process for the case study, the simulation results demonstrate the effectiveness of the developed control method.

Appendix

Proof of Theorem 1: We first show that $\boldsymbol{g}_s$ and $\boldsymbol{g}_f$ in (16) are Lipschitz continuous. According to (11), we have

$$\|\hat{\boldsymbol{y}}\|_2 = \left\| \sum_{i=1}^{M} x_i \boldsymbol{\phi}_i \right\|_2 \leq \sum_{i=1}^{M} |x_i| \|\boldsymbol{\phi}_i\|_2 \leq \eta_1 \sum_{i=1}^{M} |x_i| \tag{A.1}$$

$$\|\hat{\boldsymbol{y}}_z\|_2 = \left\| \sum_{i=1}^{M} x_i (\boldsymbol{\phi}_i)_z \right\|_2 \leq \sum_{i=1}^{M} |x_i| \, \|(\boldsymbol{\phi}_i)_z\|_2 \leq \eta_2 \sum_{i=1}^{M} |x_i| \tag{A.2}$$

$$\|\hat{\boldsymbol{y}}_{zz}\|_2 = \left\| \sum_{i=1}^{M} x_i (\boldsymbol{\phi}_i)_{zz} \right\|_2 \leq \sum_{i=1}^{M} |x_i| \|(\boldsymbol{\phi}_i)_{zz}\|_2 \leq \eta_3 \sum_{i=1}^{M} |x_i| \tag{A.3}$$

where the subscripts z stand for the partial derivatives with respect to z, $\eta_1 \triangleq \max_{i=1,\ldots,M,z\in[\underline{z},\overline{z}]} \|\boldsymbol{\phi}_i(z)\|_2$, $\eta_2 \triangleq \max_{i=1,\ldots,M,z\in[\underline{z},\overline{z}]} \|(\boldsymbol{\phi}_i(z))_z\|_2$, and $\eta_3 \triangleq \max_{i=1,\ldots,M,z\in[\underline{z},\overline{z}]} \|(\boldsymbol{\phi}_i(z))_{zz}\|_2$. Let us consider $\hat{\boldsymbol{y}}_1(z,t) = \sum_{i=1}^{M} x_{1,i}(t)\boldsymbol{\phi}_i(z)$ and $\hat{\boldsymbol{y}}_2(z,t) = \sum_{i=1}^{M} x_{2,i}(t)\boldsymbol{\phi}_i(z)$; then, it follows from (4) and (A.1)–(A.3) that

$$\begin{aligned}
&\|\boldsymbol{\mathcal{A}}(\hat{\boldsymbol{y}}_1) - \boldsymbol{\mathcal{A}}(\hat{\boldsymbol{y}}_2)\|_2 \\
&\quad \leq a_1 \|\hat{\boldsymbol{y}}_1 - \hat{\boldsymbol{y}}_2\|_2 + a_2 \|(\hat{\boldsymbol{y}}_1 - \hat{\boldsymbol{y}}_2)_z\|_2 + a_3 \|(\hat{\boldsymbol{y}}_1 - \hat{\boldsymbol{y}}_2)_{zz}\|_2 \\
&\quad \leq a_1\eta_1 \sum_{i=1}^{M} |x_{1,i} - x_{2,i}| + a_2\eta_2 \sum_{i=1}^{M} |x_{1,i} - x_{2,i}| \\
&\qquad + a_3\eta_3 \sum_{i=1}^{M} |x_{1,i} - x_{2,i}| \\
&\quad = (a_1\eta_1 + a_2\eta_2 + a_3\eta_3) \sum_{i=1}^{M} |x_{1,i} - x_{2,i}|.
\end{aligned} \tag{A.4}$$

Let $\boldsymbol{x}_1 = [x_{1,1} \ \cdots \ x_{1,M}]^{\mathrm{T}}$ and $\boldsymbol{x}_2 = [x_{2,1} \ \cdots \ x_{2,M}]^{\mathrm{T}}$. Using (12) and (A.4), then, we have

$$\begin{aligned}
&\left\| \tilde{\boldsymbol{A}}(\boldsymbol{x}_1) - \tilde{\boldsymbol{A}}(\boldsymbol{x}_2) \right\| \\
&\quad = \|\langle \boldsymbol{\mathcal{A}}(\hat{\boldsymbol{y}}_1), \boldsymbol{\Phi}(z)\rangle - \langle \boldsymbol{\mathcal{A}}(\hat{\boldsymbol{y}}_2), \boldsymbol{\Phi}(z)\rangle\| \\
&\quad = \left(\sum_{i=1}^{M} \langle \boldsymbol{\mathcal{A}}(\hat{\boldsymbol{y}}_1) - \boldsymbol{\mathcal{A}}(\hat{\boldsymbol{y}}_2), \boldsymbol{\phi}_i(z)\rangle^2 \right)^{\frac{1}{2}} \\
&\quad \leq \left(\sum_{i=1}^{M} \|\boldsymbol{\mathcal{A}}(\hat{\boldsymbol{y}}_1) - \boldsymbol{\mathcal{A}}(\hat{\boldsymbol{y}}_2)\|_2^2 \, \|\boldsymbol{\phi}_i(z)\|_2^2 \right)^{\frac{1}{2}} \\
&\quad = \left((a_1\eta_1 + a_2\eta_2 + a_3\eta_3) \sum_{i=1}^{M} |x_{1,i} - x_{2,i}| \right) \left(\sum_{i=1}^{M} \eta_1^2 \right)^{\frac{1}{2}} \\
&\quad \leq \sqrt{M}\eta_1 \left(a_1\eta_1 + a_2\eta_2 + a_3\eta_3\right) \sum_{i=1}^{M} |x_{1,i} - x_{2,i}|.
\end{aligned} \tag{A.5}$$

It is easy to verify that $\sum_{i=1}^{M}\|x_{1,i}-x_{2,i}\|$ is a norm of vector. Since all norms in the Euclidean space are equivalent, there exists a real positive constant η_4 such that $\sum_{i=1}^{M}\|x_{1,i}-x_{2,i}\| \leq \eta_4\|\boldsymbol{x}_1-\boldsymbol{x}_2\|$. Hence, it follows from (A.5) that

$$\left\|\tilde{\boldsymbol{A}}(\boldsymbol{x}_1)-\tilde{\boldsymbol{A}}(\boldsymbol{x}_2)\right\| \leq \eta_5\|\boldsymbol{x}_1-\boldsymbol{x}_2\| \tag{A.6}$$

where $\eta_5 \triangleq \sqrt{M}\eta_1\eta_4(a_1\eta_1+a_2\eta_2+a_3\eta_3)$, which means that $\tilde{\boldsymbol{A}}(\boldsymbol{x})$ is Lipschitz continuous.

Similarly, since $\boldsymbol{f}(\boldsymbol{y})$ is locally Lipschitz continuous, we have

$$\|\boldsymbol{f}(\hat{\boldsymbol{y}}_1)-\boldsymbol{f}(\hat{\boldsymbol{y}}_2)\|_2 \leq a_4\|\hat{\boldsymbol{y}}_1-\hat{\boldsymbol{y}}_2\|_2 \tag{A.7}$$

where a_4 is a real positive constant. Then, using (A.1) and (A.7), we obtain

$$\begin{aligned}\left\|\tilde{\boldsymbol{f}}(\boldsymbol{x}_1)-\tilde{\boldsymbol{f}}(\boldsymbol{x}_2)\right\| &= \|\langle \boldsymbol{f}(\hat{\boldsymbol{y}}_1)-\boldsymbol{f}(\hat{\boldsymbol{y}}_2), \boldsymbol{\Phi}(z)\rangle\| \\ &= \left(\sum_{i=1}^{M}\langle \boldsymbol{f}(\hat{\boldsymbol{y}}_1)-\boldsymbol{f}(\hat{\boldsymbol{y}}_2), \boldsymbol{\phi}_i(z)\rangle^2\right)^{\frac{1}{2}} \\ &\leq \left(\sum_{i=1}^{M}\|\boldsymbol{f}(\hat{\boldsymbol{y}}_1)-\boldsymbol{f}(\hat{\boldsymbol{y}}_2)\|_2^2\,\|\boldsymbol{\phi}_i(z)\|_2^2\right)^{\frac{1}{2}} \\ &\leq a_4\|\hat{\boldsymbol{y}}_1-\hat{\boldsymbol{y}}_2\|_2\left(\sum_{i=1}^{M}\eta_1^2\right)^{\frac{1}{2}} \\ &\leq \eta_6\|\boldsymbol{x}_1-\boldsymbol{x}_2\|\end{aligned} \tag{A.8}$$

where $\eta_6 \triangleq \sqrt{M}\eta_1 a_4$. This means that $\tilde{\boldsymbol{f}}(\boldsymbol{x})$ is Lipschitz continuous.

Therefore, $\tilde{\boldsymbol{g}}(\boldsymbol{x})$ in (13) is Lipschitz continuous, which further means that $\boldsymbol{g}_s$ and $\boldsymbol{g}_f$ in (16) are Lipschitz continuous.

Now, we prove that the closed-loop system of (12) with the optimal control $\boldsymbol{u}^*$ is asymptotically stable. From Section III-B, system (12) is equal to (16) that can be equivalently written as

$$\begin{cases}\dot{\boldsymbol{x}}_s = \boldsymbol{A}_s\boldsymbol{x}_s+\boldsymbol{B}_s\boldsymbol{u}^*+\boldsymbol{g}_s(\boldsymbol{x}_s)+[\boldsymbol{g}_s(\boldsymbol{x}_s,\boldsymbol{x}_f)-\boldsymbol{g}_s(\boldsymbol{x}_s)] \\ \varepsilon\dot{\boldsymbol{x}}_f = \boldsymbol{A}_{f\varepsilon}\boldsymbol{x}_f+\varepsilon\boldsymbol{B}_f\boldsymbol{u}^*+\varepsilon\boldsymbol{g}_f(\boldsymbol{x}_s,\boldsymbol{x}_f).\end{cases} \tag{A.9}$$

Since $Q(\boldsymbol{x}_s)$ is positive definite and $\boldsymbol{R}>0$, then there exist positive real numbers v_1, v_2, v_3, v_4, and β_1, such that, for any $\|\boldsymbol{x}_s\| \leq \beta_1$, the following conditions hold:

$$\begin{cases}v_1\|\boldsymbol{x}_s\|^2 \leq Q(\boldsymbol{x}_s) \leq v_2\|\boldsymbol{x}_s\|^2 \\ v_3\|\boldsymbol{u}^*\|^2 \leq \boldsymbol{u}^{*\mathrm{T}}\boldsymbol{R}\boldsymbol{u}^* \leq v_4\|\boldsymbol{u}^*\|^2\end{cases} \tag{A.10}$$

where $v_3 \triangleq \underline{\sigma}(\boldsymbol{R})$ and $v_4 \triangleq \overline{\sigma}(\boldsymbol{R})$.

Considering that $\mathbf{g}_s$ and $\mathbf{g}_f$ are Lipschitz continuous, then, it follows that there exist positive real numbers β_2, γ_2^*, k_1, k_2, and k_3, such that, for any $\|\boldsymbol{x}_s\| \leq \beta_2$ and $\|\boldsymbol{x}_f\| \leq \gamma_2^*$

$$\begin{cases}\|\boldsymbol{g}_s(\boldsymbol{x}_s,\boldsymbol{x}_f)-\boldsymbol{g}_s(\boldsymbol{x}_s)\| \leq k_1\|\boldsymbol{x}_f\| \\ \|\boldsymbol{g}_f(\boldsymbol{x}_s,\boldsymbol{x}_f)\| \leq k_2\|\boldsymbol{x}_s\|+k_3\|\boldsymbol{x}_f\|.\end{cases} \tag{A.11}$$

Let $\gamma_1^* \triangleq \max(\beta_1,\beta_2)$. Then, (A.10) and (A.11) hold for any $\|\boldsymbol{x}_s\| \leq \gamma_1^*$ and $\|\boldsymbol{x}_f\| \leq \gamma_2^*$.

According to the exponential stability property of the $\boldsymbol{x}_f$ subsystem (17) and the converse Lyapunov theorem [47], we have that there exist a Lyapunov function candidate V_f and positive real numbers l_1, l_2, l_3, and l_4, such that, for any $\boldsymbol{x}_f$, the following conditions hold:

$$\begin{cases}l_1\|\boldsymbol{x}_f\|^2 \leq V_f(\boldsymbol{x}_f) \leq l_2\|\boldsymbol{x}_f\|^2 \\ \dot{V}_f(\boldsymbol{x}_f) = (V_f)_{\boldsymbol{x}_f}\dot{\boldsymbol{x}}_f = (V_f)_{\boldsymbol{x}_f}\left(\left(\frac{1}{\varepsilon}\right)\boldsymbol{A}_{\varepsilon f}\boldsymbol{x}_f\right) \leq -\left(\frac{l_3}{\varepsilon}\right)\|\boldsymbol{x}_f\|^2 \\ \left\|(V_f)_{\boldsymbol{x}_f}\right\| \leq l_4\|\boldsymbol{x}_f\|.\end{cases} \tag{A.12}$$

Now, choose the smooth function

$$V(\boldsymbol{x}_s,\boldsymbol{x}_f) = V^*(\boldsymbol{x}_s)+V_f(\boldsymbol{x}_f) \tag{A.13}$$

as the Lyapunov function candidate of the system (A.9). Differentiating $V(\boldsymbol{x}_s,\boldsymbol{x}_f)$ with respect to time along the trajectories of system (A.9) and using the conditions in (A.10)–(A.12) and the optimal control (21), the following expressions can be derived:

$$\begin{aligned}\dot{V}(\boldsymbol{x}_s,\boldsymbol{x}_f) &= \dot{V}^*(\boldsymbol{x}_s)+\dot{V}_f(\boldsymbol{x}_f) \\ &= V^*_{\boldsymbol{x}_s}\left[\boldsymbol{A}_s\boldsymbol{x}_s+\boldsymbol{B}_s\boldsymbol{u}^*+\boldsymbol{g}_s(\boldsymbol{x}_s)\right] \\ &\quad +V^*_{\boldsymbol{x}_s}[\boldsymbol{g}_s(\boldsymbol{x}_s,\boldsymbol{x}_f)-\boldsymbol{g}_s(\boldsymbol{x}_s)]+(1/\varepsilon)(V_f)_{\boldsymbol{x}_f}\boldsymbol{A}_{f\varepsilon}\boldsymbol{x}_f \\ &\quad +(V_f)_{\boldsymbol{x}_f}\boldsymbol{B}_f\boldsymbol{u}^*+(V_f)_{\boldsymbol{x}_f}\boldsymbol{g}_f(\boldsymbol{x}_s,\boldsymbol{x}_f) \\ &\leq -Q(\boldsymbol{x}_s)-\boldsymbol{u}^{*\mathrm{T}}\boldsymbol{R}\boldsymbol{u}^*+k_1\|\boldsymbol{x}_f\|\|V^*_{\boldsymbol{x}_s}\| \\ &\quad -(l_3/\varepsilon)\|\boldsymbol{x}_f\|^2+l_4\|\boldsymbol{x}_f\|\|\boldsymbol{B}_f\boldsymbol{u}^*\| \\ &\quad +l_4\|\boldsymbol{x}_f\|\left(k_2\|\boldsymbol{x}_s\|+k_3\|\boldsymbol{x}_f\|\right) \\ &= -Q(\boldsymbol{x}_s)-(1/4)\left(V^*_{\boldsymbol{x}_s}\right)^{\mathrm{T}}\boldsymbol{B}_s\boldsymbol{R}^{-1}\boldsymbol{B}_s^{\mathrm{T}}V^*_{\boldsymbol{x}_s} \\ &\quad +k_1\|\boldsymbol{x}_f\|\|V^*_{\boldsymbol{x}_s}\|-(l_3/\varepsilon)\|\boldsymbol{x}_f\|^2 \\ &\quad +(l_4/2)\|\boldsymbol{x}_f\|\|\boldsymbol{B}_f\boldsymbol{R}^{-1}\boldsymbol{B}_s^{\mathrm{T}}V^*_{\boldsymbol{x}_s}\| \\ &\quad +l_4\|\boldsymbol{x}_f\|\left(k_2\|\boldsymbol{x}_s\|+k_3\|\boldsymbol{x}_f\|\right) \\ &\leq -v_1\|\boldsymbol{x}_s\|^2-(1/4)\|\boldsymbol{B}_s\boldsymbol{R}^{-1}\boldsymbol{B}_s^{\mathrm{T}}\|\|V^*_{\boldsymbol{x}_s}\|^2 \\ &\quad +k_1\|\boldsymbol{x}_f\|\|V^*_{\boldsymbol{x}_s}\|-(l_3/\varepsilon)\|\boldsymbol{x}_f\|^2 \\ &\quad +(l_4/\varepsilon)\|\boldsymbol{B}_f\boldsymbol{R}^{-1}\boldsymbol{B}_s^{\mathrm{T}}\|\|\boldsymbol{x}_f\|\|V^*_{\boldsymbol{x}_s}\| \\ &\quad +l_4\|\boldsymbol{x}_f\|\left(k_2\|\boldsymbol{x}_s\|+k_3\|\boldsymbol{x}_f\|\right) \\ &\leq -v_1\|\boldsymbol{x}_s\|^2-(v_3/4)\|V^*_{\boldsymbol{x}_s}\|^2+k_1\|\boldsymbol{x}_f\|\|V^*_{\boldsymbol{x}_s}\| \\ &\quad -(l_3/\varepsilon)\|\boldsymbol{x}_f\|^2+(l_4v_4/\varepsilon)\|\boldsymbol{x}_f\|\|V^*_{\boldsymbol{x}_s}\| \\ &\quad +l_4\|\boldsymbol{x}_f\|\left(k_2\|\boldsymbol{x}_s\|+k_3\|\boldsymbol{x}_f\|\right) \\ &= -\left[\|\boldsymbol{x}_s\|\ \|\boldsymbol{x}_f\|\ \|V^*_{\boldsymbol{x}_s}\|\right] \\ &\quad \times\boldsymbol{\Sigma}\left[\|\boldsymbol{x}_s\|\ \|\boldsymbol{x}_f\|\ \|V^*_{\boldsymbol{x}_s}\|\right]^{\mathrm{T}}\end{aligned} \tag{A.14}$$

where $v_3 \triangleq \underline{\sigma}(\boldsymbol{B}_s\boldsymbol{R}^{-1}\boldsymbol{B}_s^{\mathrm{T}})$, $v_4 \triangleq \overline{\sigma}(\boldsymbol{B}_f\boldsymbol{R}^{-1}\boldsymbol{B}_s^{\mathrm{T}})$, and

$$\boldsymbol{\Sigma} \triangleq \begin{bmatrix} v_1 & -l_4k_2/2 & 0 \\ -l_4k_2/2 & -(l_3/\varepsilon)-l_4k_3 & -(k_1+l_4v_4)/2 \\ 0 & -(k_1+l_4v_4)/2 & \frac{v_3}{4}\end{bmatrix}.$$

Defining

$$\varepsilon_1 \triangleq (4l_3v_1)/\left(4l_4k_3v_1 + l_4^2k_2^2\right)$$

$$\varepsilon_2 \triangleq (4l_3v_1v_3)\Big/\left(\left[v_1(2k_1 + l_4v_4)^2\right] + v_3(l_4k_2)^2 + 4l_4k_3v_1v_3\right)$$

and letting $\varepsilon^* \triangleq \max\{\varepsilon_1, \varepsilon_2\}$, we have that, if $\varepsilon \in (0, \varepsilon^*)$, then $\boldsymbol{\Sigma} > 0$, and thus, $\dot{V}(\boldsymbol{x}_s, \boldsymbol{x}_f) < 0$ for any $[\|\boldsymbol{x}_s\| \ \|\boldsymbol{x}_f\|]^{\mathrm{T}} \neq 0$, which implies that the closed-loop system of (16) with optimal control (30) [or (21) equivalently] is asymptotically stable, i.e., the closed-loop system of (12) is asymptotically stable. ■

Proof of Theorem 2: From (35), define

$$\tilde{H}_{i+1} \triangleq \left(\tilde{V}_{x_s}^{(i+1)}\right)^{\mathrm{T}} \left(\overline{\boldsymbol{A}}_s + \boldsymbol{B}_s \boldsymbol{u}_2^{(i)}\right) + \overline{\boldsymbol{Q}} + \left(\boldsymbol{u}_2^{(i)}\right)^{\mathrm{T}} \boldsymbol{R} \boldsymbol{u}_2^{(i)} = 0. \tag{A.15}$$

Substituting the control policy (36) into (A.15) yields

$$\tilde{H}_{i+1} = \left(\tilde{V}_{x_s}^{(i+1)}\right)^{\mathrm{T}} \left(\overline{\boldsymbol{A}}_s - (1/4)\boldsymbol{B}_s\boldsymbol{R}^{-1}\boldsymbol{B}_s^{\mathrm{T}}\tilde{V}_{x_s}^{(i)}\right) + \overline{\boldsymbol{Q}} + (1/4)\left(\tilde{V}_{x_s}^{(i)}\right)^{\mathrm{T}} \boldsymbol{B}_s\boldsymbol{R}^{-1}\boldsymbol{B}_s^{\mathrm{T}}\tilde{V}_{x_s}^{(i)}. \tag{A.16}$$

Letting $\tilde{V}^{(i+1)} = \tilde{V}^{(i)} + \Delta\tilde{V}^{(i)}$, then, it follows from (A.16) that

$$\begin{aligned}
\tilde{H}_{i+1} &= \left(\tilde{V}_{x_s}^{(i)} + \Delta\tilde{V}_{x_s}^{(i)}\right)^{\mathrm{T}} \left(\overline{\boldsymbol{A}}_s - (1/2)\boldsymbol{B}_s\boldsymbol{R}^{-1}\boldsymbol{B}_s^{\mathrm{T}}\tilde{V}_{x_s}^{(i)}\right) \\
&\quad + \overline{\boldsymbol{Q}} + (1/4)\left(\tilde{V}_{x_s}^{(i)}\right)^{\mathrm{T}} \boldsymbol{B}_s\boldsymbol{R}^{-1}\boldsymbol{B}_s^{\mathrm{T}}\tilde{V}_{x_s}^{(i)} \\
&= \Delta\dot{\tilde{V}}^{(i)} + \left(\tilde{V}_{x_s}^{(i)}\right)^{\mathrm{T}} \left(\overline{\boldsymbol{A}}_s - (1/2)\boldsymbol{B}_s\boldsymbol{R}^{-1}\boldsymbol{B}_s^{\mathrm{T}}\tilde{V}_{x_s}^{(i)}\right) \\
&\quad + \overline{\boldsymbol{Q}} + (1/4)\left(\tilde{V}_{x_s}^{(i)}\right)^{\mathrm{T}} \boldsymbol{B}_s\boldsymbol{R}^{-1}\boldsymbol{B}_s^{\mathrm{T}}\tilde{V}_{x_s}^{(i)} \\
&\quad + (1/4)\left(\Delta\tilde{V}_{x_s}^{(i-1)}\right)^{\mathrm{T}} \boldsymbol{B}_s\boldsymbol{R}^{-1}\boldsymbol{B}_s^{\mathrm{T}}\Delta\tilde{V}_{x_s}^{(i-1)} \\
&\quad - (1/4)\left(\Delta\tilde{V}_{x_s}^{(i-1)}\right)^{\mathrm{T}} \boldsymbol{B}_s\boldsymbol{R}^{-1}\boldsymbol{B}_s^{\mathrm{T}}\Delta\tilde{V}_{x_s}^{(i-1)} \\
&= \Delta\dot{\tilde{V}}^{(i)} - (1/4)\left(\Delta\tilde{V}_{x_s}^{(i-1)}\right)^{\mathrm{T}} \boldsymbol{B}_s\boldsymbol{R}^{-1}\boldsymbol{B}_s^{\mathrm{T}}\Delta\tilde{V}_{x_s}^{(i-1)} \\
&\quad + \left(\tilde{V}_{x_s}^{(i)}\right)^{\mathrm{T}} \left(\overline{\boldsymbol{A}}_s - (1/2)\boldsymbol{B}_s\boldsymbol{R}^{-1}\boldsymbol{B}_s^{\mathrm{T}}\tilde{V}_{x_s}^{(i)}\right) + \overline{\boldsymbol{Q}} \\
&\quad + (1/4)\left(\tilde{V}_{x_s}^{(i)}\right)^{\mathrm{T}} \boldsymbol{B}_s\boldsymbol{R}^{-1}\boldsymbol{B}_s^{\mathrm{T}}\tilde{V}_{x_s}^{(i)} \\
&\quad + (1/4)\left(\Delta\tilde{V}_{x_s}^{(i-1)}\right)^{\mathrm{T}} \boldsymbol{B}_s\boldsymbol{R}^{-1}\boldsymbol{B}_s^{\mathrm{T}}\Delta\tilde{V}_{x_s}^{(i-1)} \\
&= \Delta\dot{\tilde{V}}^{(i)} - (1/4)\left(\Delta\tilde{V}_{x_s}^{(i-1)}\right)^{\mathrm{T}} \boldsymbol{B}_s\boldsymbol{R}^{-1}\boldsymbol{B}_s^{\mathrm{T}}\Delta\tilde{V}_{x_s}^{(i-1)} + \tilde{H}_i.
\end{aligned} \tag{A.17}$$

Considering that $\tilde{H}_{i+1} = 0$ and $\tilde{H}_i = 0$, it follows from (A.17) that

$$\Delta\dot{\tilde{V}}^{(i)} = (1/4)\left(\Delta\tilde{V}_{x_s}^{(i-1)}\right)^{\mathrm{T}} \boldsymbol{B}_s\boldsymbol{R}^{-1}\boldsymbol{B}_s^{\mathrm{T}}\Delta\tilde{V}_{x_s}^{(i-1)} \geq 0$$

which implies that $\Delta\tilde{V}^{(i)}$ is a nondecreasing function. Since the ROM (18) is asymptotically stable, which implies that $\lim_{t\to\infty} \boldsymbol{x}_s(t) = 0$, we have $\lim_{t\to\infty} \Delta\tilde{V}^{(i)}(\boldsymbol{x}_s(t)) = 0$. Hence, we can conclude that, $\forall t \geq 0$, $\Delta\tilde{V}^{(i)} \leq 0$, i.e., $\tilde{V}^{(i)} \geq \tilde{V}^{(i+1)}$. This completes the proof of the first part of Theorem 2.

Let $\tilde{V}^{(\infty)}$ be the limit of $\tilde{V}^{(i)}$, i.e., $\tilde{V}^{(\infty)} = \lim_{i\to\infty} \tilde{V}^{(i)}$. Taking the limit for (A.16), we obtain

$$\lim_{i\to\infty}\left[\left(\tilde{V}_{x_s}^{(i+1)}\right)^{\mathrm{T}} \left(\overline{\boldsymbol{A}}_s - (1/2)\boldsymbol{B}_s\boldsymbol{R}^{-1}\boldsymbol{B}_s^{\mathrm{T}}\tilde{V}_{x_s}^{(i)}\right) + \overline{\boldsymbol{Q}} + (1/4)\left(\tilde{V}_{x_s}^{(i)}\right)^{\mathrm{T}} \boldsymbol{B}_s\boldsymbol{R}^{-1}\boldsymbol{B}_s^{\mathrm{T}}\tilde{V}_{x_s}^{(i)}\right] = 0$$

i.e., $(\tilde{V}_{\boldsymbol{x}_s}^{(\infty)})^{\mathrm{T}}\overline{\boldsymbol{A}}_s + \overline{\boldsymbol{Q}} - (1/4)(\tilde{V}_{\boldsymbol{x}_s}^{(\infty)})^{\mathrm{T}}\boldsymbol{B}_s\boldsymbol{R}^{-1}\boldsymbol{B}_s^{\mathrm{T}}\tilde{V}_{x_s}^{(\infty)} = 0$, which implies that $\tilde{V}^{(\infty)}$ solves the HJB-like equation (34). Therefore, when $i \to \infty$, $\tilde{V}^{(i)} \to \tilde{V}^*$; accordingly, $\boldsymbol{u}_2^{(i)} \to \boldsymbol{u}^*$ and $\boldsymbol{u}^{(i)} \to \boldsymbol{u}^*$. ■

References

[1] F. L. Lewis and V. L. Syrmos, *Optimal Control*. New York: Wiley, 1995.

[2] D. P. Bertsekas, *Dynamic Programming and Optimal Control*, 3rd ed. Nashua, NH: Athena Scientific, 2005.

[3] A. G. Butkovskiy, *Distributed Control Systems*. New York: American Elsevier, 1969.

[4] P. K. C. Wang and F. Tung, "Optimum control of distributed parameter systems," *J. Basic Eng.*, vol. 86, no. 1, pp. 67–79, Mar. 1964.

[5] J. L. Lions, *Optimal Control of Systems Governed by Partial Differential Equations*. New York: Springer-Verlag, 1971.

[6] H. O. Fattorini, *Infinite Dimensional Optimization Theory and Optimal Control*. Cambridge, U.K.: Cambridge Univ. Press, 1999.

[7] X. Li and J. Yong, *Optimal Control Theory for Infinite Dimensional Systems*. Boston, MA: Birkhäuser, 1995.

[8] R. F. Curtain and H. J. Zwart, *An Introduction to Infinite-Dimensional Linear Systems Theory*. New York: Springer-Verlag, 1995.

[9] I. Aksikas, A. Fuxman, J. F. Forbes, and J. J. Winkin, "LQ control design of a class of hyperbolic PDE systems: Application to fixed-bed reactor," *Automatica*, vol. 45, no. 6, pp. 1542–1548, Jun. 2009.

[10] I. Aksikas, J. J. Winkin, and D. Dochain, "Optimal LQ-feedback regulation of a nonisothermal plug flow reactor model by spectral factorization," *IEEE Trans. Autom. Control*, vol. 52, no. 7, pp. 1179–1193, Jul. 2007.

[11] W. H. Ray, *Advanced Process Control*. New York: McGraw-Hill, 1981.

[12] M. Li and P. D. Christofides, "An input/output approach to the optimal transition control of a class of distributed chemical reactors," *Chem. Eng. Sci.*, vol. 62, no. 11, pp. 2979–2988, 2007.

[13] M. Li and P. D. Christofides, "Optimal control of diffusion–convection–reaction processes using reduced-order models," *Comput. Chem. Eng.*, vol. 32, no. 9, pp. 2123–2135, Sep. 2008.

[14] C. Xu, Y. Ou, and E. Schuster, "Sequential linear quadratic control of bilinear parabolic PDEs based on POD model reduction," *Automatica*, vol. 47, no. 2, pp. 418–426, Feb. 2011.

[15] I. S. Sadek and M. A. Bokhari, "Optimal control of a parabolic distributed parameter system via orthogonal polynomials," *Optim. Control Appl. Methods*, vol. 19, no. 3, pp. 205–213, May/Jun. 1998.

[16] S. S. Ravindran, "A reduced-order approach for optimal control of fluids using proper orthogonal decomposition," *Int. J. Numer. Method Fluid*, vol. 34, no. 5, pp. 425–448, Nov. 2000.

[17] V. Yadav, R. Padhi, and S. N. Balakrishnan, "Robust/optimal temperature profile control of a high-speed aerospace vehicle using neural networks," *IEEE Trans. Neural Netw.*, vol. 18, no. 4, pp. 1115–1128, Jul. 2007.

[18] R. Padhi, S. N. Balakrishnan, and T. Randolph, "Adaptive-critic based optimal neuro control synthesis for distributed parameter systems," *Automatica*, vol. 37, no. 8, pp. 1223–1234, 2001.

[19] R. Padhi and S. N. Balakrishnan, "Proper orthogonal decomposition based optimal neurocontrol synthesis of a chemical reactor process using approximate dynamic programming," *J. Neural Netw.*, vol. 16, no. 5/6, pp. 719–728, Jun. 2003.

[20] J. Baker and P. D. Christofides, "Finite-dimensional approximation and control of nonlinear parabolic PDE systems," *Int. J. Control*, vol. 73, no. 5, pp. 439–456, 2000.

[21] J. Baker and P. D. Christofides, "Output feedback control of parabolic PDE systems with nonlinear spatial differential operators," *Ind. Eng. Chem. Res.*, vol. 38, no. 11, pp. 4372–4380, Nov. 1999.

[22] A. Armaou and P. D. Christofides, “Dynamic optimization of dissipative PDE systems using nonlinear order reduction,” *Chem. Eng. Sci.*, vol. 57, no. 24, pp. 5083–5114, Dec. 2002.
[23] H.-X. Li and C. K. Qi, *Spatio-Temporal Modeling of Nonlinear Distributed Parameter Systems: A Time/Space Separation Based Approach*. New York: Springer-Verlag, 2011.
[24] P. Holmes, J. L. Lumley, and G. Berkooz, *Turbulence, Coherent Structures, Dynamical Systems and Symmetry*. Cambridge, U.K.: Cambridge Univ. Press, 1996.
[25] L. G. Bleris and M. V. Kothare, “Low-order empirical modeling of distributed parameter systems using temporal and spatial eigenfunctions,” *Comput. Chem. Eng.*, vol. 29, no. 4, pp. 817–827, Mar. 2005.
[26] D. H. Gay and W. H. Ray, “Identification and control of distributed parameter systems by means of the singular value decomposition,” *Chem. Eng. Sci.*, vol. 50, no. 10, pp. 1519–1539, May 1995.
[27] D. G. Zheng, “System identification and model-based control for a class of distributed parameter systems,” Ph.D. dissertation, Texas Tech Univ., Lubbock, TX, 2003.
[28] B. Widrow, N. K. Gupta, and S. Maitra, “Punish/reward: Learning with a critic in adaptive threshold systems,” *IEEE Trans. Syst., Man, Cybern.*, vol. SMC-3, no. 5, pp. 455–465, Sep. 1973.
[29] J. Seiffertt, S. Sanyal, and D. C. Wunsch, “Hamilton–Jacobi–Bellman equations and approximate dynamic programming on time scales,” *IEEE Trans. Syst., Man, Cybern. B, Cybern.*, vol. 38, no. 4, pp. 918–923, Aug. 2008.
[30] H. Zhang, Q. Wei, and Y. Luo, “A novel infinite-time optimal tracking control scheme for a class of discrete-time nonlinear systems via the greedy HDP iteration algorithm,” *IEEE Trans. Syst., Man, Cybern. B, Cybern.*, vol. 38, no. 4, pp. 937–942, Aug. 2008.
[31] A. Al-Tamimi, M. Abu-Khalaf, and F. L. Lewis, “Adaptive critic designs for discrete-time zero-sum games with application to H_∞ control,” *IEEE Trans. Syst., Man, Cybern. B, Cybern.*, vol. 37, no. 1, pp. 240–247, Feb. 2007.
[32] A. Al-Tamimi, F. L. Lewis, and M. Abu-Khalaf, “Discrete-time nonlinear HJB solution using approximate dynamic programming convergence proof,” *IEEE Trans. Syst., Man, Cybern. B, Cybern.*, vol. 38, no. 4, pp. 943–949, Aug. 2008.
[33] F. L. Lewis and K. G. Vamvoudakis, “Reinforcement learning for partially observable dynamic processes: Adaptive dynamic programming using measured output data,” *IEEE Trans. Syst., Man, Cybern. B, Cybern.*, vol. 41, no. 1, pp. 14–25, Feb. 2011.
[34] H. Zhang and Y. Luo, “Neural-network-based near-optimal control for a class of discrete-time affine nonlinear systems with control constraints,” *IEEE Trans. Neural Netw.*, vol. 20, no. 9, pp. 1490–1503, Sep. 2009.
[35] D. V. Prokhorov and D. C. Wunsch, II, “Adaptive critic designs,” *IEEE Trans. Neural Netw.*, vol. 8, no. 5, pp. 997–1007, Sep. 1997.
[36] F. L. Lewis, D. Liu, and G. G. Lendaris, “Special issue on adaptive dynamic programming and reinforcement learning in feedback control,” *IEEE Trans. Syst., Man, Cybern. B, Cybern.*, vol. 38, no. 4, pp. 896–897, Aug. 2008.
[37] G. Saridis and C. S. Lee, “An approximation theory of optimal control for trainable manipulators,” *IEEE Trans. Syst., Man, Cybern.*, vol. 9, no. 3, pp. 152–159, Mar. 1979.
[38] R. W. Beard, G. N. Saridis, and J. Wen, “Galerkin approximations of the generalized Hamilton–Jacobi–Bellman equation,” *Automatica*, vol. 33, no. 12, pp. 2159–2177, Dec. 1997.
[39] R. W. Beard, G. N. Saridis, and J. Wen, “Approximate solutions to the time-invariant Hamilton–Jacobi–Bellman equation,” *J. Optimiz. Theory Appl.*, vol. 96, no. 3, pp. 589–626, Mar. 1998.
[40] M. Abu-Khalaf and F. L. Lewis, “Nearly optimal state feedback control of constrained nonlinear systems using a neural network HJB approach,” *IFAC Annu. Rev. Control*, vol. 28, no. 2, pp. 239–251, 2004.
[41] M. Abu-Khalaf and F. L. Lewis, “Nearly optimal control laws for nonlinear systems with saturating actuators using a neural network HJB approach,” *Automatica*, vol. 41, no. 5, pp. 779–791, May 2005.
[42] T. Cheng, F. L. Lewis, and M. Abu-Khalaf, “A neural network solution for fixed-final time optimal control of nonlinear systems,” *Automatica*, vol. 43, no. 3, pp. 482–490, Mar. 2007.
[43] T. Cheng, F. L. Lewis, and M. Abu-Khalaf, “Fixed-final time constrained optimal control of nonlinear systems using neural network HJB approach,” *IEEE Trans. Neural Netw.*, vol. 18, no. 6, pp. 1725–1737, Nov. 2007.
[44] M. Renardy and R. C. Rogers, *An Introduction to Partial Differential Equations*. New York: Springer-Verlag, 1993.
[45] A. J. Newman, “Model reduction via the Karhunen–Loève expansion Part II: Some elementary examples,” Inst. Syst. Res., College Park, MD, TR 96-33, 1996.
[46] J. Mercer, “Functions of positive and negative type and their connection with the theory of integral equations,” *Philos. Trans. Roy. Soc. London A, Math. Phys. Sci.*, vol. 209, no. 1909, pp. 415–446, 1909.
[47] H. K. Khalil, *Nonlinear Systems*, 3rd ed. Upper Saddle River, NJ: Prentice-Hall, 2002.
[48] P. D. Christofides and P. Daoutidis, “Finite-dimensional control of parabolic PDE systems using approximate inertial manifolds,” *J. Math. Anal. Appl.*, vol. 216, no. 2, pp. 398–420, Dec. 1997.
[49] B. A. Finlayson, *The Method of Weighted Residuals and Variational Principles*. New York: Academic, 1972.

Biao Luo received the B.E. degree in measuring and control technology and instrumentations and the M.E. degree in control theory and control engineering from Xiangtan University, Xiangtan, China, in 2006 and 2009, respectively. He is currently working toward the Ph.D. degree in control science and engineering at Beihang University (formerly Beijing University of Aeronautics and Astronautics), Beijing, China.

His current research interests include distributed parameter systems, optimal control, data-based control, fuzzy/neural modeling and control, reinforcement learning, approximate dynamic programming, and evolutionary computation.

Mr. Luo was the recipient of the “Excellent Master Dissertation Award of Hunan Province” in January 2011.

Huai-Ning Wu was born in Anhui, China, on November 15, 1972. He received the B.E. degree in automation from Shandong Institute of Building Materials Industry, Jinan, China, in 1992 and the Ph.D. degree in control theory and control engineering from Xi’an Jiaotong University, Xi’an, China, in 1997.

From August 1997 to July 1999, he was a Postdoctoral Researcher with the Department of Electronic Engineering, Beijing Institute of Technology, Beijing, China. In August 1999, he joined the School of Automation Science and Electrical Engineering, Beihang University (formerly Beijing University of Aeronautics and Astronautics), Beijing. From December 2005 to May 2006, he was a Senior Research Associate with the Department of Manufacturing Engineering and Engineering Management, City University of Hong Kong, Kowloon, Hong Kong, where he was a Research Fellow from October to December during 2006–2008 and from July to August in 2010. From July to August in 2011, he was a Research Fellow with the Department of Systems Engineering and Engineering Management, City University of Hong Kong. He is currently a Professor with Beihang University. His current research interests include robust control and filtering, fault-tolerant control, distributed parameter systems, and fuzzy/neural modeling and control.

Dr. Wu is a member of the Committee of Technical Process Failure Diagnosis and Safety, Chinese Association of Automation.